THE ROSS ICE SHELF SURVEY (RISS) 1962–1963

W. HOFMANN
Technische Hochschule, Braunschweig, West Germany

E. DORRER
Technische Hochschule, Munich, West Germany

K. NOTTARP
Bad Sodenam Taunus, Frankfort, West Germany

Part 1: General Outline and Results of the Project

W. Hofmann

The Ross Ice Shelf Survey (RISS) was planned in November 1961 by J. H. Zumberge. Under his direction, glaciological studies were made on the Ross ice shelf during the Antarctic seasons 1957–1961 [*Zumberge et al.*, 1960].

To characterize the aim of Zumberge's project it seems best to quote from his original proposal:

> '. . . . Ice shelves can be used to solve some fundamental problems of glacier flow. In formulating a satisfactory flow law for ice it is necessary to take into account the temperature of the ice and the shear stress at the glacier bed. On land glaciers we can seldom measure these things owing to the inaccessibility of the glacier bed. But on ice shelves the problem of ice flow is equivalent to that of a weightless material being compressed between frictionless plates. . . . To date we have concentrated on measuring some of the principal quantities involved in the mass balance of the Ross Ice Shelf. The 1959–1960 work aimed at a measure of the volume of ice discharged into the ocean. Twelve points were fixed by sun observations in the course of a traverse from Little America to Ross Island. . . . A pattern of stakes was set up to measure surface strain rates at 21 points across the ice shelf, and 1800 accumulation stakes were measured. With the final results of these measurements together with a measurement of surface slope, we shall be able to calculate the amount of bottom melting at points between 15 and 130 km from the ice front. . . . The research proposed herein involves the following program:
>
> '1. Remeasurement of the profile between Little America III and Ross Island. . . .'

It can be seen by this quotation that the project was mainly directed toward the determination of one important component in the mass budget of the Ross ice shelf: the ice discharge from the Ross ice front. It was to be accomplished by measurement of the temporal displacement of certain markers in a profile running approximately parallel to the ice front from Little America to Ross Island, the so-called 'Dawson trail,' named after M. Dawson who made this traverse for the first time in December 1958, marking it with cairns and poles (Figure 2). Astronomical observations (sun shots) were provided as the means of measurement.

To this project I added the proposal to use electronic distance measurement by tellurometer in combination with angle measurements instead of astronomical observations. This method was applied with full success for a similar purpose during the International Glaciological Greenland Expedition (EGIG) of 1959 under my direction [*Hofmann*, 1964]. It offered the prospect of much more accurate and reliable results. In accordance with this proposal, the new plan for RISS included a geodetic traverse along the Dawson trail.

In addition to the original project, A. P. Crary proposed the measurement of a profile running north-south along the meridian 168°W to determine the flow speed and deformation along an approximate flow line of the main influx of the Ross ice shelf coming down from Marie Byrd Land (see Figure 2).

Personnel. The RISS field party consisted of the following participants: Walther F. Hofmann, leader; Klemens Nottarp, specialist for electronic distance measurement; Egon Dorrer, geodesist, charged especially with the angle measurement; John Heap, glaciologist; William C. Campbell,

meteorologist and glaciologist; and Arthur S. Rundle, glaciologist.

Instruments. The following tellurometer sets were lent by the United States Army Corps of Engineers: master MA I-17, remote RA I-17, remote RA I-30, master + remote MRA II-3 MV, and master + remote MRA II-4 MV.

The experience of EGIG in Greenland had proved that the range of the tellurometer is significantly reduced when used over snow surfaces. Distances longer than 2–5 km could only be measured with a certain ground clearance of the measuring waves, which in Greenland was gained by placing the instruments on the roofs of vehicles (weasels). Since the RISS party had only low motor toboggans, this problem had to be solved by separating the antenna system from the body of the instrument and mount-

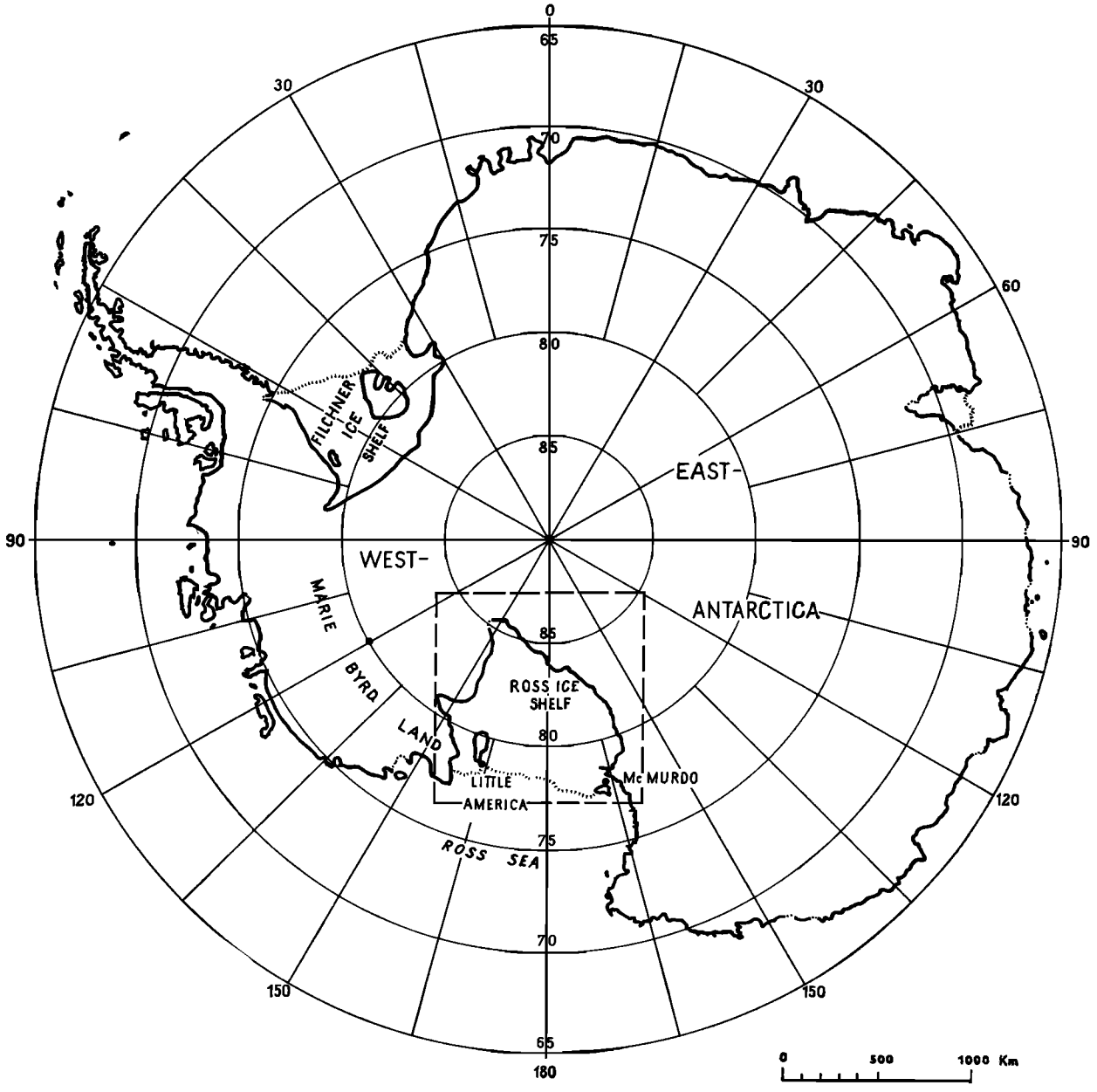

Fig. 1. Position of the Ross ice shelf in Antarctica.

ing it on aluminum poles of 4- to 5-meter height. The loss of energy in the long connecting cables had to be compensated by devices intensifying the emission. This modification of the tellurometers was devised and carried out by K. Nottarp and is described in Part 3.

For the angle measurement the RISS party had a Kern theodolite DKM 3, prepared for use under polar conditions by the manufacturer. It stood the test excellently (see Part 2). A second Wild theodolite T2 was carried along for astronomical observations, navigation, and reconnaissance. An Askania theodolite TU was used for the determination of eccentricities of the antennas only.

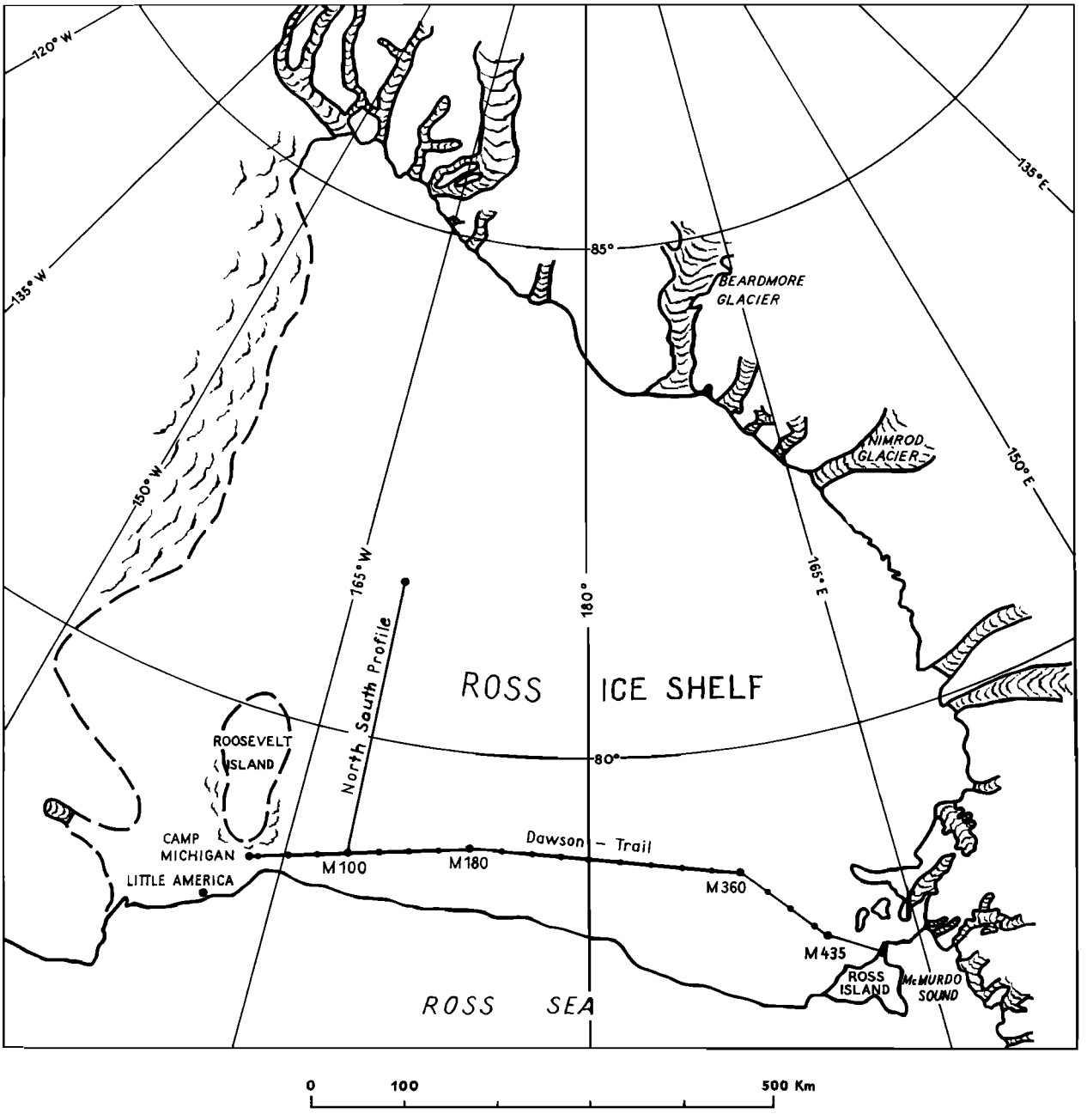

Fig. 2. Position of the RISS traverses on the Ross ice shelf.

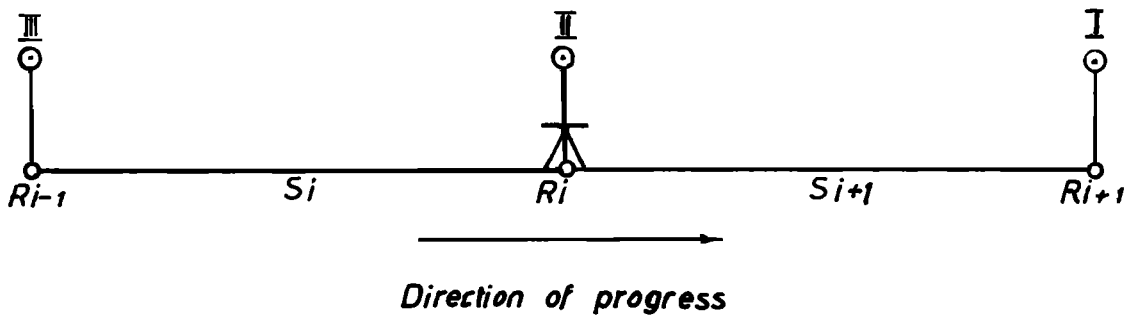

Fig. 3

Equipment. USARP placed four new Polaris Snow Traveler motor toboggans at the group's disposal for the traverse. Scientific instruments, tents, food, and motor fuel were distributed on nine Nansen sledges, two or three of which were dragged after each motor toboggan. The total payload of each toboggan train varied from 1200 to 2000 pounds.

For marking the stations aluminum poles of 62-mm diameter and 3-mm thickness were used. A single element was 1.80 meters long. Normally, the stations were marked with two elements, put together with slit collars and fixed with screwed fitting. The first element was rammed by hand in the snow surface to a depth of about 1.30 meters. After the last measurement at a certain station the second element was set up. New elements of the same type can be easily attached in the future, thus giving the poles an unlimited lifetime and making them permanent accumulation stakes.

Procedure of measurement. The planned geodetic undertaking, measurement of a traverse, necessitated the splitting of the party into three groups of two men each with the following assigned tasks (see Figure 3).

Group I: Hofmann and Rundle with 2 motor toboggans and 5 Nansen sledges, equipped with 1 tellurometer MRA II, Wild theodolite T2, and ground elements of the markers. Navigation and selection of the stations R_{i+1}. Distance measurement as the remote station backward to the previous point R_i occupied by group II.

Group II: Nottarp and Dorrer with 1 motor toboggan and 2 Nansen sledges, equipped with 1 tellurometer MA I and Kern theodolite DKM 3. Distance measurement as the master station forward to group I at R_{i+1} and backward to group III at R_{i-1}. Measurement of the angle between the stations R_{i-1} and R_{i+1}, occupied by groups I and III, in 10 sets.

Group III: Campbell and Heap with 1 motor toboggan and 2 Nansen sledges, equipped with 1 tellurometer MRA II, Askania theodolite TU, and top elements of the markers. Distance measurement as the remote station forward to point R_i occupied by group II. During the traverse: measurement of the accumulation stakes along the Dawson trail.

In this way each distance was measured twice independently. Each distance measurement consisted of 10 readings with frequency steps of 1 unit, starting from frequency 5 on the dial.

For the angle measurement the center of the high antennas at each forward and backward point was taken as the target. Its position in relation to the ground point (center of end point of the first marker element) was determined with theodolite.

Dawson had erected cairns of empty fuel drums at distances of 20 statute miles along his traverse in 1958. They were numbered from mile (M) 20 to M420 and M435 running from Little America to Ross Island. The University of Michigan traverse of 1959–1960 had linked deformation patterns to these cairns. The 20-mile points had to be included in the RISS traverse, and the strain patterns remeasured; therefore, the standard distance between two new RISS stations had to be an even part of 20 miles. In accordance with its facilities the party chose the one-fourth part, thus giving to stations a standard distance of 5 miles (8 km) along the Dawson trail. This rule was abandoned for trial only between M420 and M350, where three sections of 20 miles were bridged by three legs of 6.7 miles (10.7 km) each. When this distance turned

out to be too long, especially for the angle measurement, the party returned to the bridging with four legs of 5 miles.

With respect to the necessary glaciological work at the 20-mile points the measurement of one section between two cairns was provided and executed as one day's work.

No tie of this kind existed in the north-south profile, starting from M100. Therefore the distance of 5 minutes of arc in latitude (9.3 km) was chosen as standard distance between markers along the meridian. The party tried by precise navigation to hit points on parallels of full 5-foot values. In this section, up to 6 legs (56 km) could be measured in one day.

Control of measurement. Both distance and angle measurement was controlled by the observational procedure: double and independent distance measurement forward and backward for each leg of the traverse, and angle measurement in 10 sets at each station. If coarse errors had occurred in the tellurometer readings, they could have been detected through differences between the two values for the travel time of the measuring waves. The actual differences, which are evident in Table 3 (Part 2), are normal; they are caused by accidental observation errors and by slight changes of the travel time due to changes in the meteorological field between two measurements.

After each day's work the measurements were used for an approximate calculation of the geographical coordinates of the stations on the International Earth Ellipsoid, thus giving to the party reliable information on its position and an accurate basis for navigation. The calculation was executed with a small computing machine Curta, type II, and was extended to a numerical accuracy of 0.001 angular minute in both latitude and longitude.

The calculated coordinates were checked at several stations by sun shots, which always provided satisfactory agreement.

Log of traverse. The RISS stations are denoted with a simple number system preceded by the prefix R. The new markers at the old 20-mile points were set between Dawson's cairns and the center pole of the deformation patterns. For those markers the old denotation is given in the form Rm = Mn. The numbers are distributed as follows:

West-east profile (Dawson trail): R1 to R81 (Camp Michigan).

North-south profile: R100 = R69 = M100 to R133.

Leg to grounded ice: R200 = R77 = M59 to R201.

CHRONOLOGY OF ROSS ICE SHELF SURVEY

1962

Oct. 14: Arrival in McMurdo NAF at 05.30 local time.

Oct. 15–31: Preparation of instruments and equipment in McMurdo NAF.

Oct. 25: Measurement Camp Area-Observation Hill. Measurement of standard base line Observation Hill–Castle Rock.

Nov. 1: Start of group I from Scott Base at 15.30.

Nov. 2: Measurement Observation Hill–R1 over 24.6 km.

Nov. 3: Preparation for final start of groups II and III.

Nov. 4: Start of groups II and III from Scott Base. Meeting of the whole party at R1.

Nov. 5: Arrangement of loads. Measurement R1–R2.

Nov. 6: Measurement R2–R5 = M435; 30 km.

Nov. 7: Snowfall and blizzard. Meeting of the whole party at R5. Tellurometer frequency check.

Nov. 8: Repairs of toboggans and equipment. Measurement of deformation pattern at R5 = M435.

Nov. 9: Measurement R5–R8 = M420; 24 km.

Nov. 10: Measurement R8–R11 = M400 in 3 legs; 32 km.

Nov. 11: Measurement R11–R14 = M380 in 3 legs; 32 km.

Nov. 12: Group I starts to R15, but anomalous refraction prevents angle measurement.

Nov. 13: Measurement R14–R17 = M360 in 3 legs; 33 km.

Nov. 14: Measurement R17–R20 in 3 legs of 8 km due to difficulties with angle measurement over 10.7 km.

Nov. 15–17: Whiteout and blizzard. Groups dispersed at R21 = M340; R20 and R19.

Nov. 18: Storm calms down. Start at 09.30. Measurement R20–R22; in R22 first air supply.

Nov. 19: Measurement R22–R25 = M320; 28 km.

Nov. 20: Measurement R25–R29 = M300; 32 km.
Nov. 21: Measurement R29–R33 = M280; 32 km.
Nov. 22: Measurement R33–R37 = M260; 33 km. Passed Date Line.
Nov. 23: Measurement R37–R38; air supply in R38.
Nov. 24: Heavy wind and snow drift. Camp at R38.
Nov. 25–29: Blizzard and snowfall. Camp at R38. Tellurometer frequency check.
Nov. 30: Calming of weather, but still bad visibility. Measurement R38–R40. Again snowfall.
Dec. 1: Fog and heavy wind. Groups dispersed at R38, R39, and R40.
Dec. 2: Clearing up at noon. Measurement R40–R41 = M240.
Dec. 3: Measurement R41–R45 = M220; 32 km.
Dec. 4: Bad visibility during morning. Start 14.30; measurement R45–R47; 16 km.
Dec. 5: Measurement R47–R51, passing M200; 32 km. Air supply at R51.
Dec. 6: Measurement R51–R55, passing M180; 32 km.
Dec. 7: Measurement R55–R59, passing M160; 32 km.
Dec. 8: Measurement R59–R62, passing M140; 24 km. Trouble with carburetor of toboggan group I.
Dec. 9, 10: Fog until 15.00; start 15.30; measurement during the whole night from R62 to R69 = M100, passing M120. Arrival at M100 at 04.30, Dec. 10.
Dec. 11: Camp at M100. Tellurometer frequency check. Fog.
Dec. 12: Astronomical observations and special investigations on wave propagation at M100.
Dec. 13: Repetition of astronomical observations. Airplane with supply cannot land in whiteout conditions.
Dec. 14: Special investigations continued. Whiteout.
Dec. 15: Air supply at M100.
Dec. 16: Start in north-south profile at 09.00; measurement R100–R104; 35 km.
Dec. 17: Measurement R104–R109; 46 km.
Dec. 18, 19: Clouds, snowfall, and fog prevent measurement.
Dec. 20: Measurement R109–R115; 56 km.
Dec. 21: Measurement R115–R121; 56 km.
Dec. 22: Airplane drops Christmas mail; start 16.30; measurement R121–R124; 28 km.
Dec. 23–26: Heavy fog, later snowfall, and snow drift, storm. Groups dispersed at R122, R123, and R124.
Dec. 27: Clearing up at noon. Start 19.00; measurement R124–R129; 46 km.
Dec. 28, 29: Fog and whiteout. Repairs of toboggans. Whole party at R129.
Dec. 30: Start at midnight; measurement R129–R130; 9 km. Blizzard.
Dec. 31–Jan. 3, 1963: Snowfall, storm, and fog. Whole party camping at R130.

1963

Jan. 4: Clearing up at 14.00; start at 21.00; measurement R130–R133; 28 km. End point of north-south profile.
Jan. 5–8: Waiting for air supply at R133. Tellurometer frequency check.
Jan. 9: Air supply arrives at 14.00.
Jan. 10: Return without measurement through north-south profile. R133–R121; 112 km.
Jan. 11: Traveled R121–R109; 112 km.
Jan. 12: Traveled R109–R100 = M100; 81 km. Camp at M100.
Jan. 13–15: Waiting for air supply (aluminum tubes) at M100.
Jan. 13: Repetition of measurement R100–R101.
Jan. 16: Start in west-east profile (continued) at 09.00. Measurement R69–R73 = M80; 33 km.
Jan. 17: Measurement R73–R77 = M59; 33 km.
Jan. 18: Fog and whiteout during the morning. Air supply arrives at 14.00.
Jan. 19: After foggy morning start at 15.45. Measurement R77–R81 = Camp Michigan; 22 km.
Jan. 20, 21: Fog and whiteout. Camp at R81. Tellurometer frenquency check.
Jan. 22: Reconnaissance; visit of the old camp. Trail to Little America III blocked by new, broad crevasses.
Jan. 23: Start back westward at 09.00 along Dawson trail. From R77 = M59 trial to reach grounded ice, 30 km in southern direction. Trail blocked by heavily crevassed area after 9 km. End point marked (R201), measurement R77 = R200–R201. Return to R77. Pursuit of return to M100; arrival at 21.00.
Jan. 24: Repetition of measurement R69–R68.

TABLE 1

	Number of markers	Average distance between markers, km	Distance measured, km	Distance traveled, km
Profile west-east (Dawson trail)	81	8 3	695	800
Profile north-south	33	9 3	305	610
Total	114		1000	1410

Jan. 25: Airplane arrives from McMurdo. Transport of equipment to Roosevelt Island (Camp Wisconsin) in 2 flights. Air lift of personnel to McMurdo; arrival 23.30.

Jan. 26–28: Stay in McMurdo NAF.

Jan. 29–30: Flight to South Pole station. Establishment of a deformation pattern in quadrant 30–120. Return to McMurdo on Jan. 30, 14.15.

Jan. 31–Feb. 4: Stay in McMurdo. Computation, packing.

Feb. 5: Start with Superconstellation from McMurdo to Christchurch, New Zealand, at 09.45.

The field campaign on the Ross ice shelf lasted 86 days. Weather conditions prevented any measurements during 32 days. The unfavorable weather conditions included:

Blizzard, temporarily with snowfall	17 days
High snow drift	1 day
Fog	12 days
Abnormal refraction	2 days

A further delay of 13 days was caused by waiting for air supply or air lift. The total loss in time of 45 days reduced the available time to 41 days of measurement.

Extent and results of geodetic work. The over-all extent of the measurements in the profiles west-east (Dawson trail) and north-south are summarized in Table 1.

For glaciological purposes, only the actual distances and angles between the markers are significant. They are listed in Table 5 (Part 2). A second measurement after an adequate interval (2–3 years) will provide the change of these values and, hence, the flow speed and deformation of the ice in the profiles.

However, two distances starting from M100 and the angle between them were measured twice after a certain time interval to obtain information on the order of magnitude of the deformations expected. The results are given in Table 2.

It would be wrong to jump to conclusions about the strain distribution around point M100 on the basis of these observations separated by such short time intervals. But they make clear that after 2–3 years we can expect deformations measurable with relatively high accuracy.

The RISS traverses are tied to only two fixed points at Ross Island. The starting point is Camp Area, a triangulation point near the radio station of McMurdo NAF whose geographical coordinates were determined by the U. S. Geological Survey with astronomical means of high precision. The starting azimuth is directed from Camp Area to

TABLE 2

Leg	Date	Distance, m	Date	Distance, m	Time interval, days	Elongation, m
R101 M100	Dec. 16	6864 48	Jan. 13	6865 06	28	+0 58
M100 R69	Dec. 10	8167.19	Jan. 24	8168 11	45	+0 92

Points	Date	Angle, g	Date	Angle, g	Time interval, days	Change, cc
R101 M100 R68	Dec. 16	80.3178	Jan. 13	80.3173	28	−5

the triangulation point Crater Hill. By distance and angle measurement the triangulation point Observation Hill was connected with Camp Area. The first leg of the RISS traverse runs from the top of Observation Hill to the marker R1 over a distance of 24.6 km.

It would have been better also to connect the traverse at its eastern end to a fixed point. Such a connection was originally planned; from the north-south profile the top of Roosevelt Island should have been tied to the traverse. Lack of time, caused by bad weather and delay in support, made this connection impossible.

During the return from Camp Michigan to M100, an attempt was made to reach one of the mounds of grounded ice, discovered and described by *Crary et al.* [1962]. Group I started from station R77 in a southern direction. After a distance of 9.1 km the trail was blocked by a zone of long and big crevasses, directed east-west. Without air reconnaissance the group was not able to pass farther, and the plan had to be abandoned. However, a marker was set (station R201) and tied to R77 = R200 by angle and distance measurement. The remaining distance to the grounded ice mound was still about 20 km.

From the geodetic point of view the lack of a fixed point in the east is not a disadvantage. It would not have given any control, owing to the ice movement during the 3 months of measurement. This subject is discussed in detail in Part 2.

Part 2: Angles, Data Reduction and Coordinates

E. Dorrer

1. ANGLE MEASUREMENT

1.1 *Instruments*

Whereas all distances between neighboring stations were measured electronically, a precision Kern theodolite DKM 3 (51334) was used for the angle measurement. Its telescope magnification of 45 times and its objective aperture of 72 mm were often absolutely necessary. Besides a proper sighting telescope, an optical plumb bob, and the circle and optical micrometer graduation interval of 0.5^{cc} (centesimal seconds of arc), the very short mirror lens telescope played an important role for practical handling, for it is important to have a robust and not too delicate instrument.

The 65-cm-diameter reflectors of the tellurometer antennas, which stand 4.10 meters high when erected, were covered with black cloth and used as targets. The diameter of 65 cm corresponds to an angle of 50^{cc} at a normal distance of 8 km, having therefore the same order of magnitude as the parallactic angle defined by both vertical threads of the telescope reticle. Because the mirages varied at all times, the low setting of the theodolite (1.0–1.5 meters above surface) proved very unfavorable. Surprisingly, however, the inextensible Kern tripod guaranteed an unobjectionable and stable connection with the snow surface.

1.2 *Measuring Process*

Three groups followed each other at a distance of about 8 km apart. The middle group set the theodolite, by means of the optical plumb bob, vertically above the center of the upper end of an aluminum tube (Figure 4), 1.80 meters long and 62 mm in diameter. This center defines the reference point to which all measurements were later related. It normally stood clear of the snow surface by about 50 cm.

Since mainly horizontal sights occurred, it was sufficient to observe the target in *one* position without 'plunging' the telescope. To accelerate the whole procedure, the tubes were not placed in the snow exactly vertically. Both remote groups (groups I and III) therefore had to measure the horizontal deflection of the reflector center against the reference point lateral to the traverse. This measurement was made by setting up a theodolite at a distance of about 10 meters in the direction of the traverse sight, plumbing the reflector center, and measuring the eccentricity Ex (Figure 5) at a ruler held out by the second man. During distance measurement, this value had to be transmitted on the voice frequency of the tellurometer system, and it was written down in a special form for registration of angles (Figure 6).

Having found both targets, the observer at the theodolite brought the graduated circle into zero position, when looking toward the backward station, and started the angle measurement. In order to avoid tripod torsion and sinking into snow, it was well understood from the very outset that every traverse angle had to be measured as quickly

as possible. The plan was to measure every angle by 10 repetitions, in order to compensate systematic errors of circle graduation and to increase accuracy. The micrometer was brought in coincidence three times at each target bearing; the graduated circle was turned approximately 40^g (centesimal grads) after each repetition. The writer recorded all readings with an accuracy of 1^{cc} on a special form (Figure 6) with copy, computed the mean values and the proper angles, their expectation value and standard deviation. Having received the eccentricities from the other groups, he was then able to calculate a corresponding angle correction ϵ according to $\epsilon = Ex \cdot \rho/s$ (Figure 7) and correct the traverse angle (Figure 6).

1.3 *Accuracy*

Using 118 observations, a mean square error for angle measurement of $\pm 2.4^{cc}$, at a dispersion range from 0.8^{cc} to 8.4^{cc}, was found for the whole traverse. This value still contains a systematic part of the error of circle graduation (2.3.1). Eliminating it, the mean angle error becomes $\pm 2.3^{cc}$. The biggest errors occur mainly at the very beginning of the traverse, being caused by poor acclimation of the observer, ignorance of special observation methods on the ice, and unsatisfactory co-ordination between the three groups during the first days. Future RISS expeditions will have to consider these factors.

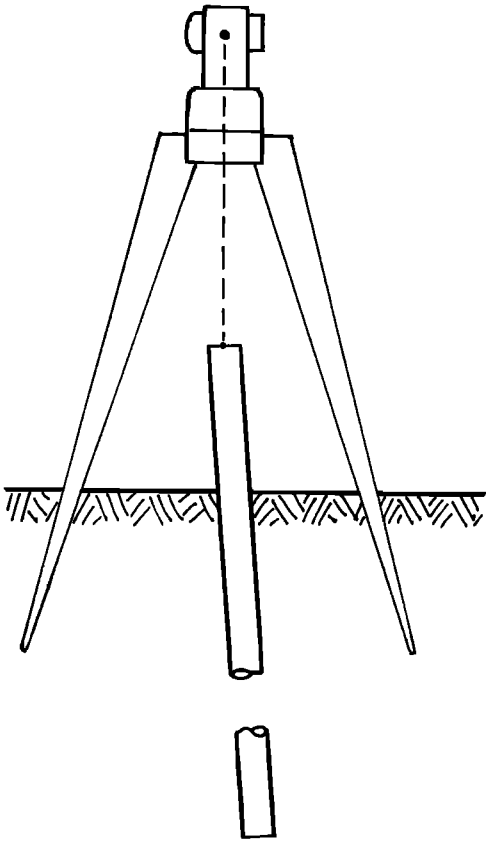

Fig. 4. Theodolite vertically above reference point.

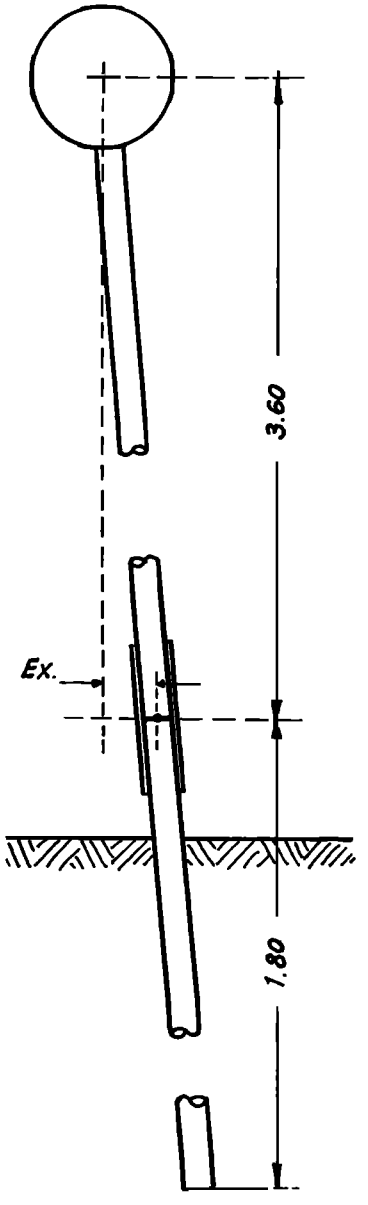

Fig. 5. Eccentricity of the target.

Standpunkt: RISS 20 Datum: 17.11.62, 1800 Beob. EGON IH = e = 0

S.	Ziel	I	II	1	2	3	M	Mittel		Richtung		v	vv	Bem., Skizze
	R.19	0:0:0	2.8	8:1	7:9	8:0	8:0	200	3:9:22	200	3:9:23	+1	1	Exzentrizitäten
	R.21	200:0	6:8	0:0	0:3	0:2	0:2							cm (cc)
		0:4:0	3:1	8:4	8:7	8:9	8:7	200	3:9:20			+3	9	-2 -1.5
		240	7:1	0:6	0:7	0:8	0:7							+3 +2.7
		0:8:0	1:8	6:7	6:7	6:7	6:7	200	3:9:23			0	0	+12^cc = +1^cc
		280	5:7	8:9	9:1	9:0	9:0							
		1:2:0	2:8	8:0	8:6	8:4	8:3	200	3:9:24			-1	1	
		320	6:8	0:6	0:9	0:7	0:7							
		1:6:0	4:0	7:1	6:8	6:8	6:9	200	3:9:15			+8	64	200.3923
		360	7:9	8:2	8:5	8:4	8:4							+1
		1:99	8:8	1:8	1:7	1:8	1:8	200	3:9:26			-3	9	200 3924
		0:0:0	2:7	4:1	4:4	4:6	4:4							
		2:4:0	5:5	0:1	0:2	0:2	0:2	200	3:9:24			-1	1	
		040	9:4	2:6	2:5	2:7	2:6							
		2:8:0	1:0	0:9	0:8	1:0	0:9	200	3:9:26			-3	9	
		0:8:0	4:9	3:5	3:5	3:6	3:5							
		3:2:0	4:3	8:1	8:2	8:1	8:1	200	3:9:29			-6	36	
		120	8:3	0:9	1:2	0:9	1:0							
		3:59	8:1	3:6	3:6	3:6	3:6	200	3:9:17			+6	36	
		1:60	2:0	5:4	5:3	5:3	5:3							
								3	9:2:26			+4	166	m = ± 1.3^cc

Fig. 6. Form for registration of angles.

1.4 *Environmental Influences*

In polar regions, external influences upon angle measurement are of a peculiar character. The most important ones are discussed below.

1.4.1 *Scintillation.* This is a well-known property of the lower atmosphere over hot objects in warmer climates [*Miller,* 1963]. As a characteristic of increasing temperature gradient and decreasing mass balance of the air [*Geiger,* 1961], it also occurs above radiated snow and ice areas. The targets seem to move up and down and from one side to the other randomly, so that sighting is difficult and nerve-racking.

1.4.2 *Disturbing background.* If there is a dark or snow-free hill in the background, the normally excellent target contrast decreases and the targets perish by scintillation. Remedy: Artificial light source or heliostat.

1.4.3 *Atmospheric refraction and mirage.* Probably caused by high increase of the temperature gradient above the snow surface, the slightly inclined light beam will be totally reflected upward. Normally, one can always see two targets, one on the other (Figures 8 and 9). Their vertical separation depends on the magnitude of temperature gradient and on the instrument height above surface. Both targets overflow and finally vanish (Figure 8), if the instrument lies below a certain minimum height. Remedy: Wait until temperature gradient decreases, or set up the instrument on a higher level (higher tripod, on the top of a vehicle). Because of such abnormal atmospheric refraction, vertical angles must not be observed without knowing exactly the temperature layers. In flat terrain, horizontal refraction lies below the threshold value of measurement; it may, however, assume observable values in hilly or mountainous terrain. *Brocks* [1954] shows a way to determine temperature gradients by optical means.

1.4.4 *Topography.* More than two superjacent targets refer to an undulating surface ('transition zone,' at the beginning of the RISS traverse [*Stuart* and *Bull,* 1963]). The main difficulty on a horizontal surface is Earth curvature which, at a distance of 8 km, already comes to 5 meters height difference (Figure 8). Slight height undulations and surface slopes can be seen by the eye only after some experience. In a few cases, the 8-km interval had

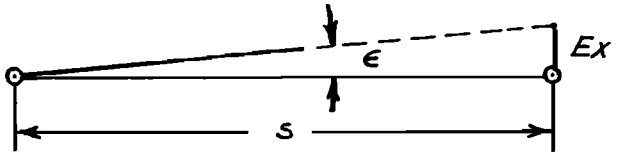

Fig. 7

to be given up in order to set up the traverse stations at the highest points of undulations.

1.4.5 *Weather in general.* With clear sky, increasing air movement causes twinkling and waving of the targets to some degree, so that direct and reflected image can no longer be distinguished. At a wind speed of 6 m/sec or more, scintillation decreases quickly. Much higher velocities give rise to snow drift, which makes observations difficult or impossible. Although extraordinarily favorable conditions for angle observation exist during overcast whiteout [*Kasten,* 1960] (extremely contrasting and stable targets, high sighting accuracy), there is great risk and danger in moving in a universal 'light swamp.' It is, for instance, almost impossible to employ helicopters.

1.4.6 *Observer and chill.* Since the observer adjusts to the cold climate only slowly, he must especially protect his face and fingers. Normally, gloves are not sufficient. Thick mittens were used without any reduction in the accuracy of observation. Sightings against wind and a low sun are troublesome, as search for the target, sighting, and reading require rather a long time.

2. DATA REDUCTION

2.1 *General*

Independently from all reductions performed on the ice, each tellurometer measurement has been reduced numerically at home. Owing to the partly complicated formulas and the large number of observations, the problem was programmed in Algol and calculated by an electronic computer. As opposed to the tellurometer observations, nearly all angles were measured in such a way that their mean values could immediately be compensated for errors of circle graduation and alidade eccentricity. Being incomplete only in a few instances, this small part of observations had to be corrected for errors of circle graduation (2.3.2).

2.2 *Reduction of Tellurometer Measurements*

2.2.1 *Field data.* All transmission times are taken directly out of the field notes, as are dry-bulb and wet-bulb air temperatures, barometric pressure, and eccentricity. All station heights are related to the center of the reflector. The traverse heights above sea level are taken from *Crary* [1962], the heights of Observation Hill (H = 747 ft = 227.7 m) and Castle Rock (H = 1355 ft = 444 m) from the chart 'NAF McMurdo and Vicinity, H.O.6712, 1st edition.'

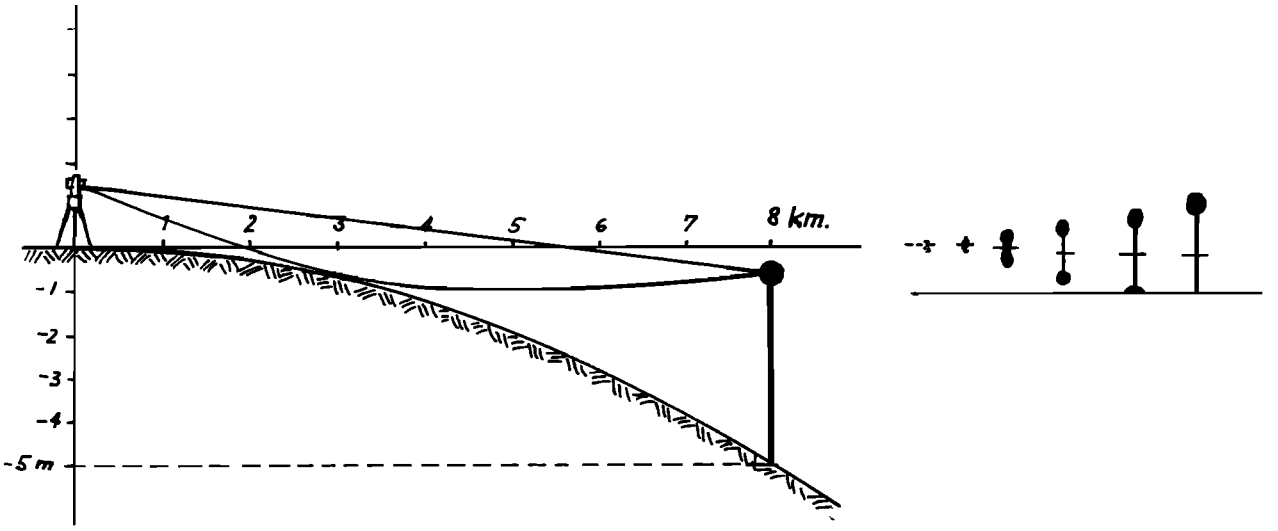

Fig. 8. Mirage downward. View through theodolite.

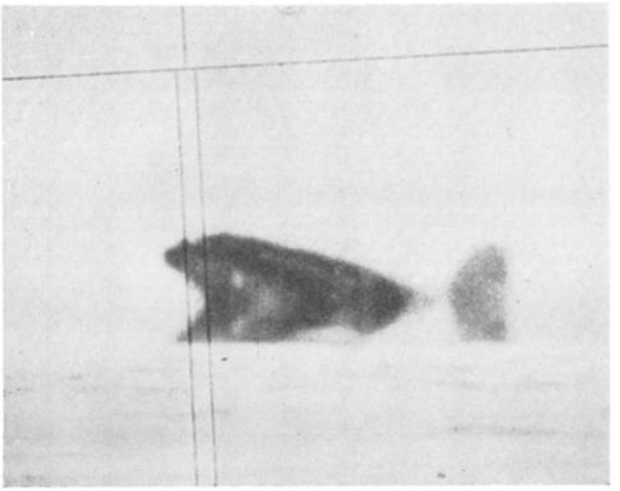

Fig. 9. Telephoto of an airplane at a distance of 8 km.

Vertical angle measurements were necessary only between the stations 'Camp Area' (—1), 'Observation Hill' (0), and R1 (1). At all other stations on the ice shelf, vertical angle measurements would have been illusory anyhow, because of the abnormal refraction conditions. Assuming a completely horizontal surface, the height difference between neighboring stations is 2 meters because the antenna of the master station (group II) was only 2.5 meters high. The height difference causes a slope distance differing from its horizontal distance by, at most, 1 mm, which is negligible in the accuracy of observation.

Table 3 contains all data necessary for reduction of the tellurometer measurements. In detail, the numbered columns imply:

Col. 1: Number of the master station (group II).

Col. 2: Number of the remote station (group I or III). C.R. = *Castle Rock,* nail on the top plateau. C.A. = *Camp Area,* starting station in McMurdo (USGS). O.H. = *Observation Hill,* bench mark.

Col. 3: Transmission time of tellurometer waves, normally the mean of 10 individual measurements.

Col. 4: Air temperature, mean of the dry-bulb thermometer readings at both stations.

Col. 5: Wet-bulb depression, difference between dry- and wet-bulb temperature.

Col. 6: Barometric pressure, mean of the aneroid barometer readings at both stations and, after reduction, to a stationary barometer in McMurdo.

Col. 7: Distance eccentricity, sum of the two eccentricities at both stations.

Col. 8: Altitude above sea level of the reflector at master station.

Col. 9: Altitude above sea level of the reflector at remote station.

Col. 10: Distance difference between forward and backward measurement. Already partial result of computations.

2.2.2 *Reduction formulas.* The basic formula to determine distances by transmission times measured with tellurometer is

$$s = c_0 t/2n$$

where s = distance, c_0 = velocity of propagation of electromagnetic waves in vacuo, t = transmission time, and n = index of refraction in air. The standard value for the velocity in vacuo (visible light and radio microwaves) which has been adopted by the International Union of Geodesy and Geophysics is

$$c_0 = 299,792.5 \pm 0.4 \text{ km/sec}$$

All the following computations are based on that value.

The index of refraction in air is mainly a function of barometric pressure, air humidity, and air temperature. These three parameters being scalar functions and varying with time, the index of refraction should theoretically be known at all points of the radio wave beam. In practice, this demand can never be met. Instead one must be content with the measurement of all necessary meteorological data at both stations, taking the mean values as representative for the whole distance.

For the index of refraction in air, a formula according to Essen-Froome is currently assumed to be the best. It is

$$n = 1 + \frac{10^{-6}}{T} \cdot \left[103.49\, P + \left(\frac{0.4958 \cdot 10^6}{T} - 17.23 \right) (P_e - 0.00066\, dT\, P) \right]$$

where T = absolute temperature in °K, P = barometric pressure in torrs, dT = wet-bulb depression in °C, P_e = saturated water vapor pressure in torrs. P_e as function of temperature (here valid only over ice) can be computed by the formula

TABLE 3. Data for Reduction of Tellurometer Measurements

Stations		LZ, 10^{-9} sec	t, °C	Δt, °C	P, mb	ex, m	Altitudes, m		Δs, m
1	2	3	4	5	6	7	8	9	10
C. R.	O. H.	40,227 70	−16 9	8	931 7	− 13	444	228 6	− 036
O. H.	C. R.	40,227 48	−17.5	8	932 1	−.13	228 6	444	
C. A.	O. H.	5,085 22	−17 4	1.1	955 2	+ 04	51 9	228 6	+ 073
O. H.	C. A.	5,085 70	−17 4	.9	955 0	+.04	228 6	51 9	
O. H.	R1	164,539 28	−15 6	.0	979 9	−1 54	229	28	+ 186
R1	O. H.	164,540 60	−15 6	.0	979.9	−1 54	26	229	
R1	R2	51,230.10	−24 9	0	987 9	− 13	26	29	+ 107
R2	R1	51,230.10	−18 8	1	984 6	− 07	27	28	
R2	R3	54,517.62	−19.1	.0	984 0	+ 03	27	29	− 034
R3	R2	54,516.92	−18.3	.2	984 0	+ 09	27	29	
R3	R4	47,323 65	−18.2	2	984 0	− 07	27	31	−.232*
R4	R3	47,321 79	−19 2	.2	984 2	− 02	29	29	
R4	R5	47,987.18	−18 9	.2	983 8	−.04	29	33	−.069
R4	R5	47,986 78	−18 0	.3	986 7	− 04	29	33	
R5	R6	54,185.65	−17 2	.5	984 8	+.07	31	36	+ 020
R6	R5	54,186.08	−16.7	.3	985.5	+ 03	34	33	
R6	R7	54,649.18	−16.3	.2	984.3	+.02	34	40	−.012
R7	R6	54,649 55	−15 0	.4	984 9	−.06	38	36	
R8	R7	54,208.12	−14 4	.2	985 0	−.05	42	40	+ 009
R8	R7	54,208 18	−14.4	.2	985.0	− 05	42	40	
R8	R9	64,855.05	−20.6	.0	984.5	+ 09	42	50	−.040
R9	R8	64,855.00	−17.4	.2	985.0	+.03	48	44	
R9	R10	72,983.43	−17.8	.1	983.8	−.22	48	55	−.045
R10	R9	72,938.10	−16 8	.1	984.7	−.22	53	50	
R10	R11	79,419.65	−17.0	.1	983 1	−.03	53	59	+.007
R11	R10	79,419 85	−20.9	.3	984.6	−.03	57	55	
R11	R12	70,942.42	−19.8	.2	984.6	+ 03	57	60	−.164
R12	R11	70,941.55	−17 0	.0	985.3	−.01	58	59	
R12	R13	70,580 42	−16.8	.0	984.5	+.07	58	61	− 005
R13	R12	70,580.65	−17.0	.3	985.3	+.02	59	60	
R13	R14	77,063.70	−16 7	.4	985 0	−.09	59	61	− 033
R14	R13	77,064.20	−19.2	.2	985.4	−.17	59	61	
R14	R15	75,982.35	−21.1	.0	984.2	+ 07	59	60	−.110
R15	R14	75,980.85	−15 1	.3	974 9	+.10	58	61	
R15	R16	70,841 32	−16.1	.2	973.8	−.03	58	60	−.171
R16	R15	70,840 78	−20.1	.1	974.3	− 09	58	60	
R16	R17	72,214.28	−19 8	.0	973.3	−.18	58	59	−.047
R17	R16	72,213 45	−20 6	.3	973.2	− 11	57	60	
R17	R18	55,576.18	−19 6	.0	968.8	+.03	57	58	+ 019
R18	R17	55,575.70	−17 5	.0	968 6	+.11	56	59	
R18	R19	55,062 20	−17.2	.0	968.2	+ 10	56	57	+.038
R19	R18	55,062.38	−20 6	.0	968.8	+ 13	55	58	
R20	R19	54,663.55	−22 5	.0	968.9	−.17	55	57	+.015
R20	R19	54,662.98	−14.6	.1	973.0	−.10	55	57	
R20	R21	52,987.05	−14.8	.1	972.3	+.02	55	56	−.092
R21	R20	52,987 38	−17.5	.0	984 0	−.08	54	57	
R21	R22	33,026.42	−17.8	.3	984 2	−.09	54	56	+.040
R22	R21	33,025 45	−16 7	.0	984.8	+ 10	54	56	
R22	R23	60,781.42	−18 3	.0	990.3	−.05	54	55	+.029
R23	R22	60,780.98	−16.3	.0	992.0	+.04	53	56	
R23	R24	62,174.75	−15 9	.0	991.3	+ 05	53	55	−.020
R24	R23	62,174 32	−16 4	.2	991 9	+.09	53	55	
R24	R25	62,328.52	−16.8	.0	991.4	.00	53	55	+.057
R25	R24	62,328.30	−15.5	.0	989.9	+ 08	53	55	
R25	R26	55,697 68	−14 2	.2	989.6	+.04	53	55	−.048
R26	R25	55,698 00	−12.9	.0	990.4	− 05	53	55	
R26	R27	55,075.85	−13.1	.1	990.1	− 03	53	55	+.058
R27	R26	55,076 40	−13 7	.0	990.1	− 05	53	55	
R27	R28	54,652 05	−13.8	.0	990.0	.00	53	55	+.107
R28	R27	54,652.72	−13.9	.2	990.2	.00	53	55	

TABLE 3. (Continued)

Stations		LZ, 10^{-9} sec	t, °C	Δt, °C	P, mb	ex, m	Altitudes, m		Δs, m
1	2	3	4	5	6	7	8	9	10
R28	R29	52,470.78	−13.5	.0	989.9	−.01	53	55	−.069
R29	R28	52,470 50	−14.9	.0	991.4	−.03	53	55	
R29	R30	56,643.90	−14.5	.0	991.0	−.01	53	55	+.017
R30	R29	56,643.92	−13.1	.3	991.4	−.01	53	55	
R30	R31	54,577 10	−12.8	.2	991 0	+ 02	53	55	+ 029
R31	R30	54,577.45	−12.7	.1	991.1	.00	53	55	
R31	R32	51,707 32	−12.7	0	990.9	+.03	53	55	+.043
R32	R31	51,707.78	−13.2	.1	990 3	.00	53	55	
R32	R33	56,411.68	−13.2	.1	988.7	−.12	53	55	−.063
R33	R32	56,411 92	−13.0	.1	987.6	−.09	53	55	
R33	R34	55,501.80	−12.0	.3	987.0	+.05	53	55	+.034
R34	R33	55,502 52	−13.0	.2	987.6	−.02	53	55	
R34	R35	55,088.22	−12.2	.3	987.2	−.07	53	55	−.054
R35	R34	55,088 00	−13 3	.1	987.9	−.08	53	55	
R35	R36	53,911.40	−12.7	.4	987.3	+.08	53	54	+.036
R36	R35	53,911.72	−13.5	.4	987.1	+.07	52	55	
R36	R37	54,121.08	−13.1	.5	986 6	+.02	52	54	−.096
R37	R36	54,121.10	−18 9	.0	986.6	−.04	52	54	
R37	R38	41,199.71	−17.6	0	985.4	+.08	52	54	+.031
R38	R37	41,200.78	−17 3	.0	985 3	−.05	52	54	
R38	R39	67,903 45	−7.8	0	994.7	−.04	52	54	+.044
R39	R38	67,904.60	−8.1	.0	994.2	−.17	52	54	
R39	R40	60,442.75	−8 3	.0	993.8	+.02	52	54	−.016
R40	R39	60,442.95	−10.8	0	981.2	−.06	52	54	
R40	R41	48,533.38	−10.6	0	980.9	− 04	52	54	+.019
R41	R40	48,533.52	−12 3	.0	981.0	−.04	52	54	
R41	R42	55,193 00	−11.8	1	971 6	+ 05	52	54	−.144
R42	R41	55,192 92	−11.8	.0	970 8	−.08	52	54	
R42	R43	54,319.35	−11.9	.0	970.4	−.02	52	54	−.018
R43	R42	54,319.18	−13 5	2	969.3	−.02	52	54	
R43	R44	55,203.62	−13.4	2	968.8	−.06	52	54	− 070
R44	R43	55,202.85	−14.7	.1	968.1	−.01	52	54	
R44	R45	53,808 52	−14.8	0	967.7	−.05	52	54	+.068
R45	R44	53,808.75	−13.8	.0	967.1	−.02	52	54	
R45	R46	55,762.62	−13 5	.0	967.3	.00	52	54	+.093
R46	R45	55,763.05	−13.8	0	967.6	+.03	52	54	
R46	R47	54,611 00	−14.1	0	967.4	−.03	52	54	+.051
R47	R46	54,611.98	−13 8	.0	967 9	−.08	52	54	
R47	R48	52,341.55	−7.3	.2	968.8	−.06	52	55	−.053
R48	R47	52,341 60	−7.1	.0	969.8	−.11	53	54	
R48	R49	56,110.32	−7 3	.0	969.4	+.03	53	55	+ 012
R49	R48	56,110.42	−7.4	.0	970.0	+.04	53	55	
R49	R50	55,415.55	−7.2	.0	969.5	−.12	53	55	−.008
R50	R49	55,415.45	−6 6	.0	970.2	−.05	53	55	
R51	R50	54,579.35	−8.9	0	970.4	+.11	54	55	
R51	R52	47,832.40	−10.4	.0	969.6	−.06	54	56	+.069
R52	R51	47,832.35	−10.5	0	970.0	+ 05	54	56	
R52	R53	61,044.85	−10.2	.0	969.4	− 01	54	56	+ 042
R53	R52	61,044 60	−10.3	0	969.4	+.07	54	56	
R53	R54	54,930.60	−9.4	.0	968 8	−.18	54	56	−.122
R54	R53	54,928.92	−9.8	0	968.9	−.05	54	56	
R54	R55	55,101.40	−9.3	.0	968 4	+.08	54	56	+.022
R55	R54	55,100.68	−9.3	0	968.7	+.21	54	56	
R55	R56	54,707 25	−9.6	.0	967.7	−.13	54	56	+.018
R56	R55	54,707.28	−6.5	.1	969.8	−.11	54	56	
R56	R57	54,551.70	−7.9	.1	969.7	−.05	54	56	+.061
R57	R56	54,551.10	−8.6	.2	971.1	+.10	54	56	
R58	R57	55,705.40	−9 1	.0	972 4	+.05	54	56	
R58	R59	55,107.00	−9.2	.0	972.6	+.03	54	56	−.019
R59	R58	55,106.52	−10.0	.1	973.4	+.08	54	56	
R59	R60	54,223.25	−5 0	.0	981.4	−.09	54	57	+ 051
R60	R59	54,223.45	−4.9	.3	982.0	−.08	55	56	

TABLE 3. (Continued)

Stations		LZ, 10^{-9} sec	t, °C	Δt, °C	P, mb	ex, m	Altitudes, m		Δs, m
1	2	3	4	5	6	7	8	9	10
R60	R61	54,692 75	−4.8	.2	981 8	− 04	55	57	− 010
R61	R60	54,692.10	−7 0	0	982.8	+.05	55	57	
R61	R62	54,785 25	−4 7	0	982 0	+ 04	55	57	+ 087
R62	R61	54,785 65	−7.2	.0	983.0	+ 06	55	57	
R62	R63	50,296 75	−6.6	0	980.9	+ 06	55	57	− 036
R63	R62	50,296.92	−6 1	.0	981 0	.00	55	57	
R63	R64	64,228.50	−8 9	.0	980 7	−.04	55	58	− 065
R64	R63	64,228 82	−7.0	.0	980 4	− 15	56	57	
R64	R65	50,013.40	−7 8	0	980.1	−.09	56	58	− 093
R65	R64	50,012 25	−7.5	.0	980.1	− 01	56	58	
R65	R66	52,637.80	−8.0	.0	979 8	+ 03	56	58	−.036
R66	R65	52,637.30	−7.8	.0	980 0	+.07	56	58	
R66	R67	57,129.60	−7.9	0	979 3	−.15	56	58	− 072
R67	R66	57,128.52	−8.2	.0	979.2	−.06	56	58	
R67	R68	54,793 15	−8.3	.0	978 8	+.03	56	59	+.016
R68	R67	54,792.58	−9.8	.0	979.2	+.13	57	58	
R68	R69	54,502.50	−9.7	.0	979.1	−.08	57	59	+.073
R69	R68	54,502.42	−10.2	.0	979.0	+.02	57	59	
R69	R101	45,809 75	−7.5	.0	978.2	−.16	57	60	+.058
R101	R69	45,808.88	−5 9	.0	977.1	+.03	58	59	
R101	R102	48,159.50	−6 5	.1	977.5	+.12	58	61	−.038
R102	R101	48,159.00	−6.6	.0	977.7	+.16	59	60	
R102	R103	67,884.30	−6 8	.0	977.3	+.01	59	62	+ 022
R103	R102	67,884.78	−7.4	.0	977.9	−.04	60	61	
R104	R103	73,966 00	−7.8	.0	978.2	−.07	61	62	+.053
R104	R103	73,966.38	−6.6	.0	981.5	−.06	61	62	
R104	R105	57,650.19	−6.5	.0	981.1	+.01	61	64	+.215*
R105	R104	57,650.88	−7.2	.0	981.3	+.12	62	63	
R105	R106	62,921.95	−7.6	.1	981.1	−.01	62	65	−.015
R106	R105	62,921.48	−7.9	.0	981.5	+.05	63	64	
R106	R107	62,053.90	−8.2	.0	981.2	+.06	63	66	−.018
R107	R106	62,054.18	−8.5	.0	981.5	.00	64	65	
R107	R108	61,687.60	−8 6	0	980.5	−.02	64	66	−.088
R108	R107	61,687.42	−9.1	.0	981.0	−.08	64	66	
R108	R109	62,764.45	−9.1	.0	980 9	+.04	64	67	+.001
R109	R108	62,764.40	−8.5	.0	981 3	+ 05	65	66	
R109	R110	62,125 45	−8.7	.0	974.4	−.05	65	67	+.020
R110	R109	62,125.85	−8.2	.0	977.6	−.08	65	67	
R110	R111	63,965 50	−8.1	.0	977.6	+.13	65	68	−.022
R111	R110	63,965.88	−9.1	.0	978.0	+.05	66	67	
R111	R112	62,428.90	−9.3	.0	977.8	+ 05	66	69	+.050
R112	R111	62,430.45	−12.0	.0	978.4	− 13	67	68	
R112	R113	61,686.30	−11.6	.0	978.2	−.04	67	69	+ 024
R113	R112	61,687.08	−12.5	.0	978 8	−.13	67	69	
R113	R114	61,519.20	−12.0	.0	978.5	+.01	67	70	−.047
R114	R113	61,519.18	−12 5	.0	979.6	−.03	68	69	
R114	R115	59,554.00	−11.8	.0	979 4	−.02	68	70	−.008
R115	R114	59,554.05	−8.8	.0	985 4	− 02	68	70	
R115	R116	64,676.50	−9.2	.0	985.0	+.07	68	70	+.004
R116	R115	64,676.75	−10.7	.0	986 3	+.04	68	70	
R116	R117	62,868 25	−11.4	.0	986.0	+.01	68	70	+.081
R117	R116	62,869.48	−12 4	.0	986 7	−.09	68	70	
R117	R118	62,832.60	−13.5	.0	986.5	−.12	68	70	+.032
R118	R117	62,832.68	−14.4	.1	987.2	−.10	68	70	
R118	R119	61,117.25	−14.3	.0	987.2	+.12	68	70	+.062
R119	R118	61,117.52	−14.3	.3	987 5	+.13	68	70	
R119	R120	58,600.65	−14.5	.0	987.9	−.04	68	70	+.002
R120	R119	58,600.92	−15.2	.1	988.0	−.08	68	70	
R120	R121	64,094 15	−15.0	.0	987.9	+.09	68	69	−.083
R121	R120	64,093.85	−13.9	.0	988.3	+.05	67	70	
R121	R122	62,825.30	−9.5	.0	990.5	+.04	67	69	+.002
R122	R121	62,826.25	−10.8	.2	990 3	−.11	66	69	

TABLE 3. (Continued)

Stations		LZ, 10^{-9} sec	t, °C	Δt, °C	P, mb	ex, m	Altitudes, m		Δs, m
1	2	3	4	5	6	7	8	9	10
R122	R123	64,243 85	−11 4	0	990 1	+ 01	66	66	+ 009
R123	R122	64,244.72	−13.4	.1	990.4	−.11	64	68	
R123	R124	61,708.50	−14 0	0	990 2	+.03	64	65	+ 274*
R124	R123	61,710 28	−8 5	.0	974.2	− 01	63	66	
R124	R125	59,372.55	−9.7	.0	974.1	− 15	63	64	+ 076
R125	R124	59,372.80	−10 2	.0	974 5	−.11	62	65	
R126	R125	61,755 42	−13 0	0	974 5	+ 18	62	64	
R126	R127	62,877.85	−13.0	.0	973.8	+ 03	62	63	− 040
R127	R126	62,877.98	−13 5	0	973.2	−.03	61	64	
R127	R128	62,622 55	−13.5	0	973 0	+ 02	61	63	− 067
R128	R127	62,621.95	−12.5	.0	972 9	+.04	61	63	
R128	R129	62,895 95	−11 4	.0	972.6	− 02	61	63	+ 015
R129	R128	62,896.40	−8.7	.0	973.0	−.07	61	63	
R129	R130	61,574.65	−7.2	.0	988.8	+.08	61	63	+ 072
R130	R129	61,575 55	−5.7	0	987 8	+.02	61	63	
R131	R130	61,926 90	−7.8	.0	990.9	− 08	62	63	
R131	R132	63,466 75	−7.8	0	990 8	00	62	65	+.006
R132	R131	63,467 50	−9 3	.0	990 4	− 11	62	65	
R132	R133	63,508.90	−11.0	.0	989.8	− 02	63	66	− 020
R133	R132	63,509.28	−9.8	.0	989 0	− 10	64	65	
R69	R101	45,812 65	−4 0	0	969 6	00	57	60	
R69	R68	54,508.60	−10.1	.0	976.0	− 04	57	59	
R69	R70	58,659 25	−9 0	.0	967.8	+.18	57	59	− 029
R70	R69	58,659 00	−9 4	.0	968 5	+.19	57	59	
R70	R71	54,884 05	−9.2	0	967.9	− 01	57	59	− 089
R71	R70	54,884 00	−8.9	0	968 2	− 09	57	59	
R71	R72	52,651.65	−9.1	.0	967.6	+ 08	57	58	− 078
R72	R71	52,652.15	−8.3	.0	968 0	− 07	56	59	
R72	R73	57,829 30	−8.5	0	967 7	−.11	56	58	− 067
R73	R72	57,828 98	−9 6	0	967 8	−.13	56	58	
R73	R74	56,361.90	−8.5	.0	966 2	+ 09	56	56	+ 016
R74	R73	56,361.75	−8 0	.0	966 2	+.13	54	58	
R74	R75	54,761 55	−7.6	0	966 3	+ 09	54	53	− 085
R75	R74	54,762.00	−7 4	.0	966.2	− 06	51	56	
R75	R76	60,884 20	−7.6	0	966 0	+ 16	51	50	− 003
R76	R75	60,885.88	−6.6	0	966.3	− 09	48	53	
R76	R77	49,392.90	−6 8	.0	966.0	− 07	48	45	− 137
R77	R76	49,393 42	−6.6	.0	966 5	−.28	43	50	
R77	R78	52,260.30	−11.3	.0	978 6	− 06	43	42	+ 018
R78	R77	52,260 25	−12 8	0	979 2	− 03	40	45	
R78	R79	52,691 30	−13.1	0	979.4	+ 01	40	40	+ 031
R79	R78	52,691 22	−15 0	0	979 9	+ 06	38	42	
R79	R80	21,197.50	−15 5	.0	980 0	+ 14	38	37	− 064
R80	R79	21,197.85	−17.0	.0	980 8	+.03	35	40	
R80	R81	20,518.80	−17 3	0	981 0	− 07	35	33	+ 354*
R81	R80	20,521 60	−17 3	0	981 5	− 13	31	37	
R77	R201	60,743.15	−8.2	0	981.0	−.10	43	50	

* Values that exceed the allowable mean square error.

according to Goff-Gratch [*Smithsonian Meteorological Tables*, 1939]:

$$P_r(t) = 4.58 \cdot 10^{-9.09718[273.16/(273.16+t)-1]} \cdot 10^{-3.56654 \cdot lg(273.16/273.16+t)} \cdot 10^{+0.876793[1-(273.16+t)/273.16]}$$

where t = wet-bulb temperature in °C.

For all field data, listed in Table 3, the index of refraction and also the slope distance was computed for each traverse distance by

$$s = (LZ\ 0.14989625/n) + Ex$$

where LZ = transmission time in 10^{-9} sec, Ex = eccentricity in meters. These direct distances s on the surface of the ice shelf will be

required for the later comparison with RISS 2, in order to determine the deformation. For computing the traverse, however, reduction of all distances to sea level is recommended. Denoting R as earth radius within the surveying region, and H_1, H_2 as heights of two neighboring traverse stations above sea level, then

$$s_r = 2R \arcsin \left[\frac{1}{2} \sqrt{\frac{(s + H_2 - H_1)(s - H_2 + H_1)}{(R + H_1)(R + H_2}} \right]$$

is the reduced distance of s. The Algol program used these formulas to compute all traverse distances of RISS 62–63. The results are listed in Table 6.

2.3 *Reduction of Angles*

2.3.1 *Errors of circle graduation.* Each graduation mark on the graduated circle deviates from its ideal position, specified by a number, by a small amount composed of a random and a systematic part. The systematic part describes a periodic function that can be represented by a Fourier series. Dependent on the location φ on the graduated circle, the periodic error of circle graduation is

$$F(\varphi) = \sum_{i=0}^{\infty} a_i \sin (i\varphi + \alpha_i)$$
$$= \sum_{i=0}^{\infty} (x_i \sin i\varphi + y_i \cos i\varphi)$$

where a_i, α_i, and x_i, y_i are constants.

A measured angle ω will be falsified by two errors, namely at φ and $\varphi + \omega$. If we put

$$F(\varphi + \omega) - F(\varphi) = \Delta F(\varphi, \omega)$$

then an 'angle graduation error' is

$$\Delta F(\varphi, \omega) = \sum_{i=0}^{\infty} ((\sin i(\varphi + \omega) - \sin i\varphi)x_i$$
$$+ (\cos i(\varphi + \omega) - \cos i\varphi)y_i$$

2.3.2 *Actual conditions at RISS 62–63.* The period of $F(\varphi)$ with respect to $\Delta F(\varphi,\omega)$ of the theodolite DKM 3 ('double circle') is exactly $2\pi = 400^g$. Because a great majority of angles of the RISS traverse are 200^g (including those not completely observed), it is possible to approximate statistically the function

$$\Delta F(\varphi, \pi) = -2 \cdot \sum_{i=0}^{\infty} [x_{2i+1} \sin (2i + 1)\varphi$$
$$+ y_{2i+1} \cos (2i + 1)\varphi]$$

TABLE 4. Error of Circle Graduation

Position, φ	$\Delta F(\varphi, \pi)$		$\frac{\Delta F(\varphi, \pi) - \Delta F(\varphi + \pi, \pi)}{2}$	
0^g	$-0\ 5^{cc}$		$0\ 0^{cc}$	
40	$+2\ 1$		$+2.1$	
80	$+2\ 8$		$+2\ 4$	
120	$+0\ 6$		$+0.5$	
160	$+4\ 3$		$+3\ 9$	
200	$-0\ 4$	$\pm 0\ 43^{cc}$	$0\ 0$	$\pm 0\ 3^{cc}$
240	$-2\ 0$		$-2\ 1$	
280	$-1\ 9$		-2.4	
320	$-0\ 4$		$-0\ 5$	
360	$-3\ 6$		$-3\ 9$	

at the ten used positions of the graduated circle. The equation

$$\Delta F(\varphi, \pi) = -\Delta F(\varphi + \pi, \pi)$$

provides an important control of the method. In order to compute $\Delta F(\varphi,\pi)$, all the stations were used whose traverse angle has a standard deviation m less than 2.0^{cc}. All corrections v (Figure 6) were then given a weight of 1 for $2.0^{cc} \geqq m \geqq 1.5^{cc}$ and of 2 for $1.4^{cc} \geqq m \geqq 0.8^{cc}$. Based on the results from 59 stations, the mean values of all v for the ten positions on the graduated circle and their mean square error are listed in Table 4. See also Figure 10.

Thus, all incompletely observed traverse angles at the stations R4, R55, and R130 could be corrected for errors of circle graduation. Angle 4 had no correction, angles 55 and 130 each 1^{cc}. A complete list of all traverse angles is given in Table 5.

The error of circle graduation gives a mean square deviation of $\pm 0.7^{cc}$, thus reducing the originally calculated mean square error of the angle measurement (cf. 1.3) from 2.4^{cc} to 2.3^{cc}.

3. COMPUTATION OF COORDINATES

3.1. *Principle*

Given are traverse data. All traverse stations are situated on an ice body which moves relative to the system of geographical coordinates on the Earth ellipsoid; therefore, the positions of all traverse stations, as well as the measured distances and angles, are dependent on time. Hence all distances and angles must be reduced to a reference time. With so little known about the movement of the Ross ice shelf, the observed traverse has to be treated like a rigid, undeformable traverse, which means

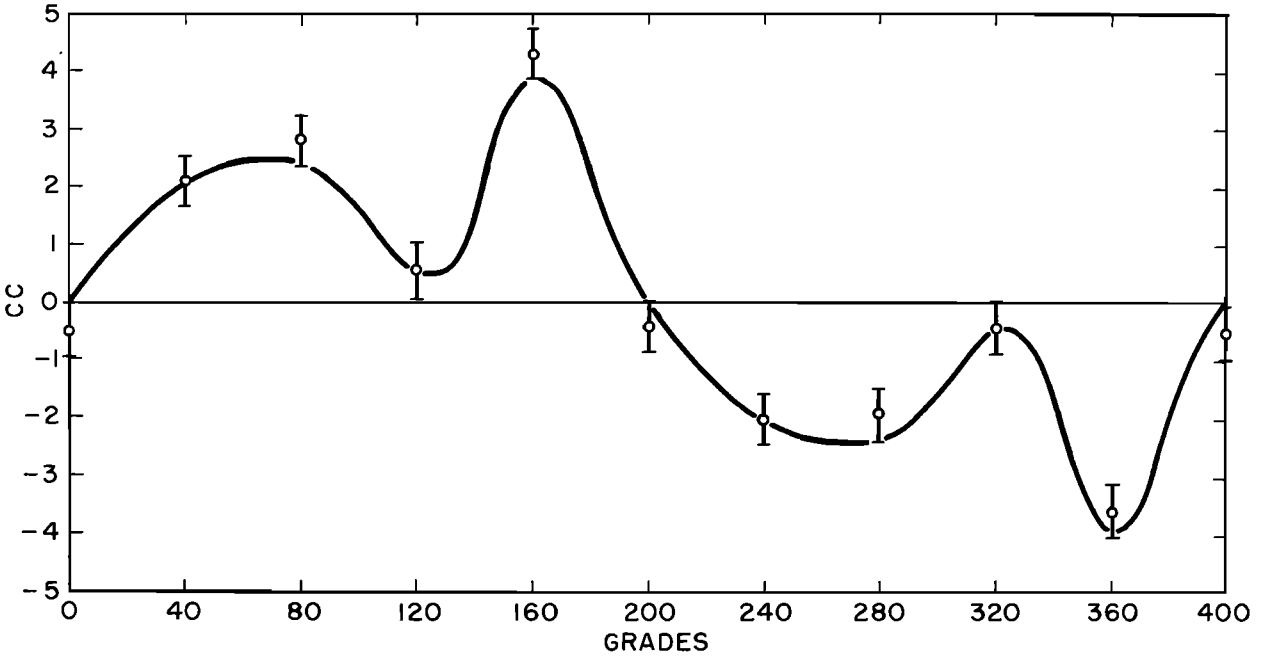

Fig. 10. Influence of the error of circle graduation and alhidade eccentricity upon an angle of 200^g (DKM 3, 51334).

all field data are assumed to be independent of time. This assumption is no doubt wrong, for both distances and angles changed during the observation period (see Table 2). When considered rigid, the traverse will be systematically deformed by computation (Figure 11; cf. also 3.4). Therefore, geographical coordinates calculated with the RISS data can be only approximate and do not meet rigid geodetic standards. However, considering the relatively slight deformations during the period of measurement (3 months), those coordinates are accurate enough for navigation and tracing of the markers in the future.

In the case of RISS, geographical coordinates at the International Earth Ellipsoid were computed for all stations, using a new numerical method. It solves the three first-order differential equations of the geodetic of any rotation ellipsoid:

$$\lambda' = \frac{d\lambda}{ds} = \frac{\sin\alpha}{a\cdot\cos\varphi}\sqrt{U}$$

$$\varphi' = \frac{d\varphi}{ds} = \frac{\cos\alpha}{a(1-f)^2}\,U\cdot\sqrt{U}$$

$$\frac{d\alpha}{d\lambda} = \sin\varphi$$

with $U = 1 - f(2 - f)\sin^2\varphi$ by means of an iterative process according to Runge-Kutta. This method is the topic of another paper.

3.2 *Data for Computation*

3.2.1 *Initial data.*

International Ellipsoid:

Radius of equator	6,378,388 m
Flattening	0.003367003367

Coordinates of the first station 'Camp Area':

Longitude (east)	+166°40′13″.8
Latitude (south)	—77°50′52″.5

Azimuth from Camp Area to Crater Hill (true north): 57.9769^g.

3.2.2 *Reduced field data.* All angles required for calculating coordinates may be found in Table 5. The horizontal distances are listed in Table 6.

3.3 *Sequence of Calculations*

Starting at McMurdo, Camp Area, there were computed, in turn, the geographical coordinates (λ_{i+1}, φ_{i+1}) and the backward azimuth α'_{i+1} of the station P_{i+1} from its preceding station P_i (Figure 12) with known longitude λ_i, latitude φ_i, backward azimuth α_i', measured traverse angle ω_i, and traverse distance s_{i+1}. An Algol program of this prob-

TABLE 5. Actual Distances and Polygon Angles in the RISS Profiles West-East (Dawson Trail) and North-South

Column 1, station; column 2, mileage from Observation Hill; column 3, measured distance s' between stations; column 4, polygon angles β; column 5, date of measurement during RISS 1962–1963.

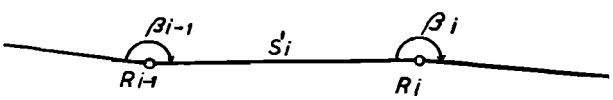

Profile West-East (Dawson Trail)

1	2	3	4	5
Station	km	s_i', m	β_i, g	Date
O. H.	0		162.2909	
		24,654 77		11/02
R1	24.65		198.2507	
		7,676.68		11/06
R2	32.33		199.7177	
		8,169.45		11/06
R3	40.50		196.8289	
		7,091.24		11/06
R4	47.59		202.0073	
		7,190.79		11/07
R5	54.78		235.9436	
		8,119.79		11/09
R6	62.90		200.0132	
		8,189.18		11/09
R7	71.09		199.8038	
		8,123.03		11/09
R8	79.21		199.6829	
		9,718.55		11/10
R9	88.93		200.5057	
		10,929.55		11/10
R10	99.86		200.3037	
		11,900 98		11/11
R11	111.76		199.5042	
		10,630.63		11/11
R12	122.39		200.3104	
		10,576.51		11/11
R13	132.97		200.1339	
		11,547.87		11/12
R14	144.52		199.6041	
		11,385.91		11/12
R15	155.91		200.3500	
		10,615.47		11/13
R16	166.53		200.2255	
		10,821.09		11/13
R17	177.35		163.2823	
		8,328.13		11/14
R18	185.68		199 6915	
		8,251.21		11/14
R19	193 93		199.7975	
		8,191.16		11/15
R20	202.12		200.3924	
		7,940.10		11/16
R21	210.06		199.2693	
		4,948.93		11/18
R22	215.01		200.4873	
		9,108.02		11/19
R23	224.12		200.0053	
		9,316.89		11/19

TABLE 5. (Continued)

1	2	3	4	5
Station	km	s_i', m	β_i, g	Date
R24	233.44		200.1109	
		9,339 91		11/20
R25	242.78		199.7882	
		8,346.30		11/20
R26	251.13		199.9471	
		8,253 10		11/20
R27	259 38		200.1917	
		8,189.64		11/20
R28	267 57		200 1293	
		7,862.68		11/21
R29	275 43		199.8644	
		8,488 06		11/21
R30	283.92		200.1813	
		8,178 40		11/21
R31	292 10		200.0336	
		7,748.37		11/21
R32	299.85		199.7685	
		8,453.18		11/21
R33	308 30		200.3847	
		8,317.01		11/22
R34	316.62		199.8515	
		8,254.87		11/22
R35	324.87		199.9403	
		8,078.72		11/22
R36	332.95		199.9389	
		8,110.02		11/23
R37	341.06		199.9004	
		6,173 86		11/23
R38	347.23		200.1483	
		10,175.28		11/30
R39	357.41		200.2639	
		9,057.34		12/01
R40	366 47		200.0196	
		7,272.71		12/02
R41	373.74		198.3211	
		8,270.69		12/03
R42	382.01		199.8709	
		8,139.76		12/03
R43	390.15		200.0627	
		8,272.22		12/03
R44	398 42		199.9183	
		8,063.23		12/04
R45	406.48		200.1633	
		8,356.12		12/04
R46	414.84		199.9071	
		8,183.54		12/04
R47	423.02		199.9740	
		7,843.34		12/05
R48	430.86		200.0190	
		8,408.22		12/05
R49	439.27		199.4687	
		8,304.00		12/05
R50	447.57		199.9712	
		8,178.87		12/05
R51	455.75		199.9824	
		7,167.73		12/06
R52	462.92		200.0358	
		9,147.63		12/06
R53	472.07		179.0629	
		8,231.15		12/06

TABLE 5. (Continued)

1	2	3	4	5
Station	km	s_i', m	β_i, g	Date
R54	480 30		199.4512	
		8,257.08		12/06
R55	488.56		200.0891	
		8,197 81		12/07
R56	496.76		199.9352	
		8,174.60		12/07
R57	504 93		210 4301	
		8,347.54		12/07
R58	513.28		199 9682	
		8,257.84		12/07
R59	521.54		199.9883	
		8,125.29		12/08
R60	529.67		199.8508	
		8,195.68		12/08
R61	537.87		199.8845	
		8,209.66		12/08
R62	546.08		200.0228	
		7,537.01		12/09
R63	553 62		199.9008	
		9,624 59		12/09
R64	563.24		200.1715	
		7,494.39		12/09
R65	570.73		199.9094	
		7,887.80		12/10
R66	578 62		199.9282	
		8,560.71		12/10
R67	587.18		200.0397	
		8,210.81		12/10
R68	595.39		200.1032	
		8,167.19		12/10
R69 = M100	603.56		199.9157	
		8,790.31		01/16
R70	612 35		200 0650	
		8,224.38		01/16
R71	620.57		200.0678	
		7,889 94		01/16
R72	628.46		200.1032	
		8,665 64		01/16
R73	637.13		200 1050	
		8,445.99		01/17
R74	645.58		200.0855	
		8,206.12		01/17
R75	653.79		207.6496	
		9,123 72		01/17
R76	662.91		228 2440	
		7,401 44		01/17
R77	670 31		169 6696	
		7,831.18		01/19
R78	678.14		204.6804	
		7,895.84		01/19
R79	686.04		157.5487	
		3,176.56		01/19
R80	689.22		209.9232	
		3,075.03		01/20
R81 = Camp Michigan	692.30			
		Profile North-South		
R100 = R69	0		319.6822	
		6,864 48		12/16

TABLE 5. (Continued)

1	2	3	4	5
Station	km	s_i', m	β_i, g	Date
R101	6.86		200 6640	
		7,216.83		12/16
R102	14 08		200.3037	
		10,172.52		12/16
R103	24.25		197.6538	
		11,083.80		12/17
R104	35.33		202.1099	
		8,639.02		12/17
R105	43.97		200.3440	
		9,428.86		12/17
R106	53.40		197.7558	
		9,298.85		12/17
R107	62.70		204.4670	
		9,243.85		12/17
R108	71 94		196.9064	
		9,405.32		12/17
R109	81.35		195.0824	
		9,309.50		12/20
R110	90.66		210.3514	
		9,585.38		12/20
R111	100.25		192.6984	
		9,355.08		12/20
R112	109.61		200.2448	
		9,243.70		12/20
R113	118.85		203.0741	
		9,218.67		12/21
R114	128.07		198 6592	
		8,924.17		12/21
R115	136.99		200.7944	
		9,691.86		12/21
R116	146 68		193 5944	
		9,420.87		12/21
R117	156.10		211.1365	
		9,415.37		12/21
R118	165.52		194.6733	
		9,158.57		12/22
R119	174.68		192.2012	
		8,781.27		12/22
R120	183.46		210.7482	
		9,604.56		12/22
R121	193.06		197.7925	
		9,414.41		12/22
R122	202 47		193 6070	
		9,626 96		12/22
R123	212.10		210 0164	
		9,247.18		12/25
R124	221.35		194.5466	
		8,896.91		12/27
R125	230 25		209.1651	
		9,254.26		12/28
R126	239.50		186 0659	
		9,422.30		12/28
R127	248.92		201.5759	
		9,384.02		12/28
R128	258 30		211.9438	
		9,425.00		12/28
R129	267.72		186.9663	
		9,227.08		12/30
R130	276.95		201.7199	
		9,279.67		01/02

TABLE 5. (Continued)

1	2	3	4	5
Station	km	s_i', m	β_i, g	Date
R131	286.23		204 3025	
		9,510.50		01/05
R132	295.74		196 7194	
		9,516 79		01/05
R133	305 26			
	Leg to Grounded Ice			
R77 = R200	670 31			
		9,102 34	276 0828	01/23
R201	679.41			

lem had been established, and the RISS traverse was calculated by the Perm computer of the Technische Hochschule München. The results are listed in Table 6.

3.4 *Estimation of Errors*

In contrast to the mean square error quotable directly for every angle, the error of distance can be determined only by the various double measurements. All differences between backward and forward distance, listed in Table 3, column 10, give a mean square error of ±0.032 meter for the mean of any distance measured twice, and of ±0.047 meter

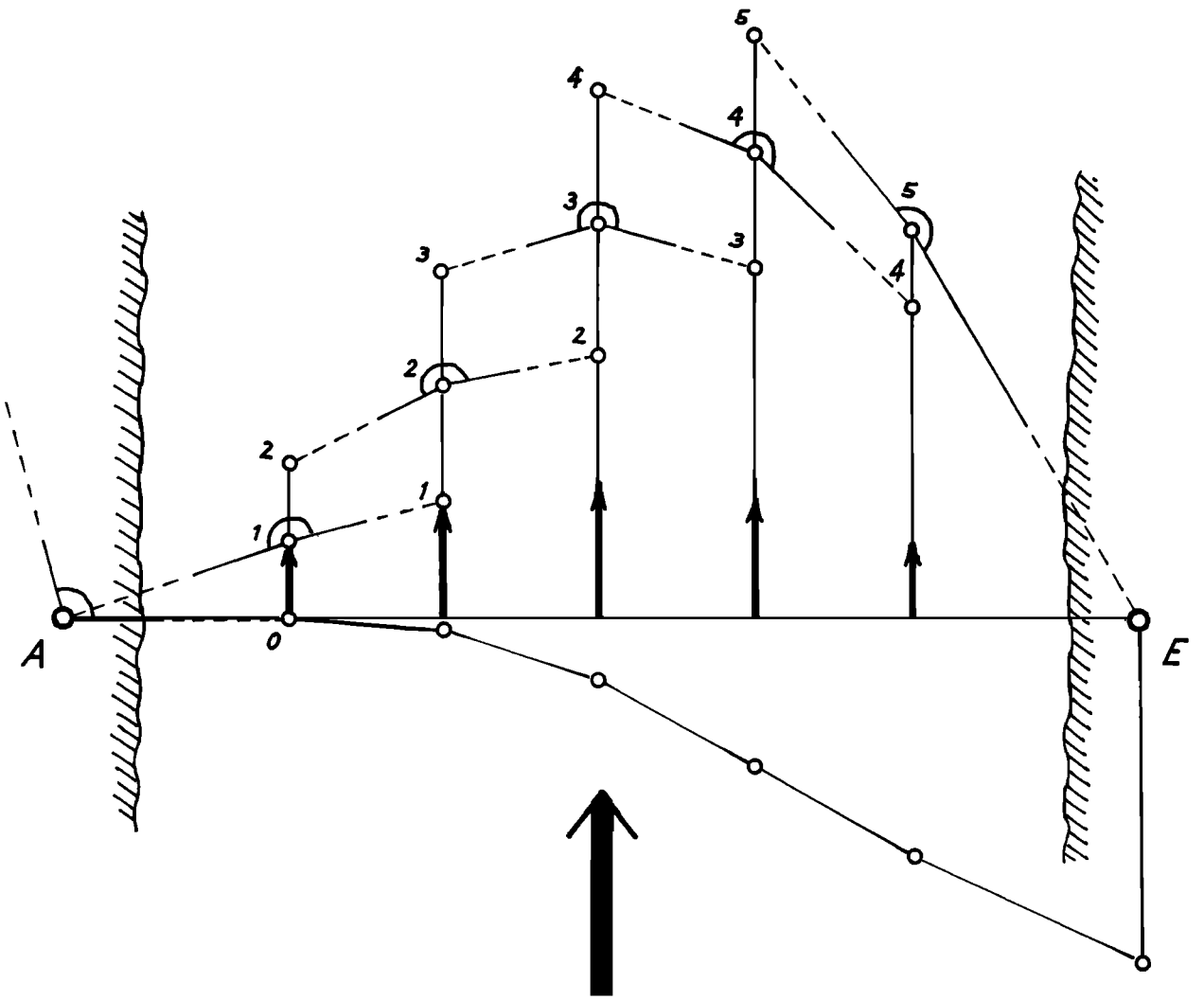

Fig. 11. Influence of ice movement upon a traverse.

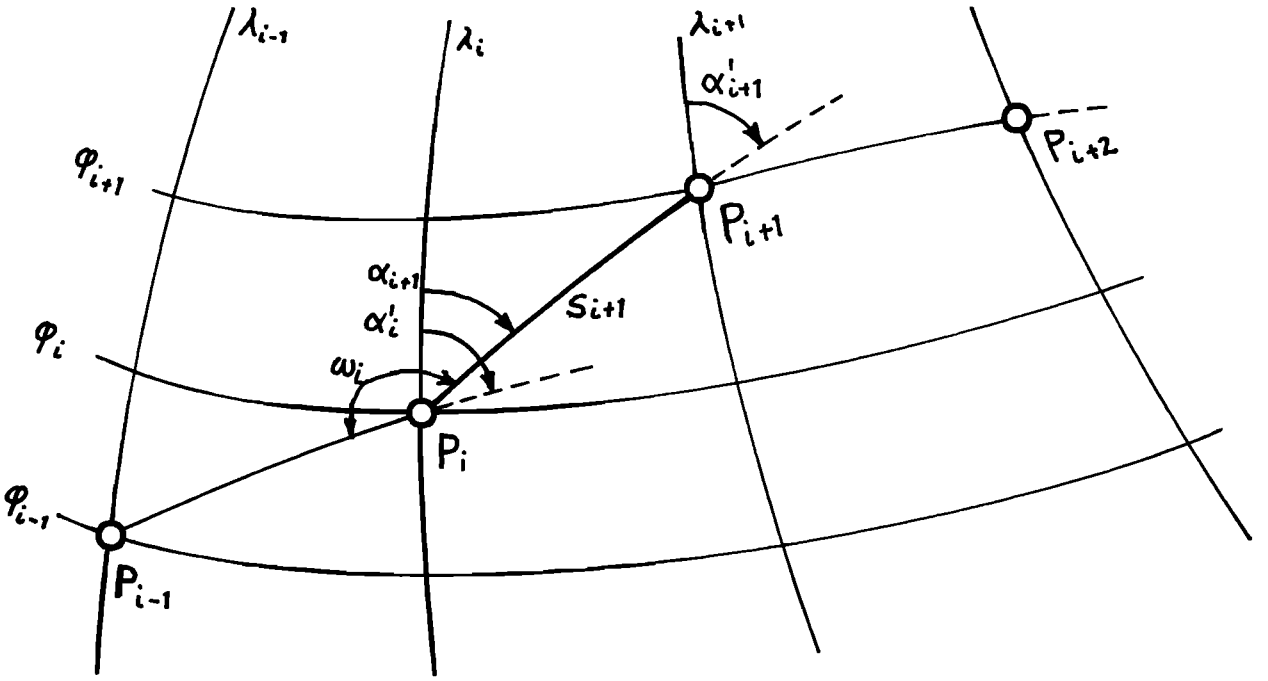

Fig. 12. Traverse point transfer from P_i to P_{i+1}

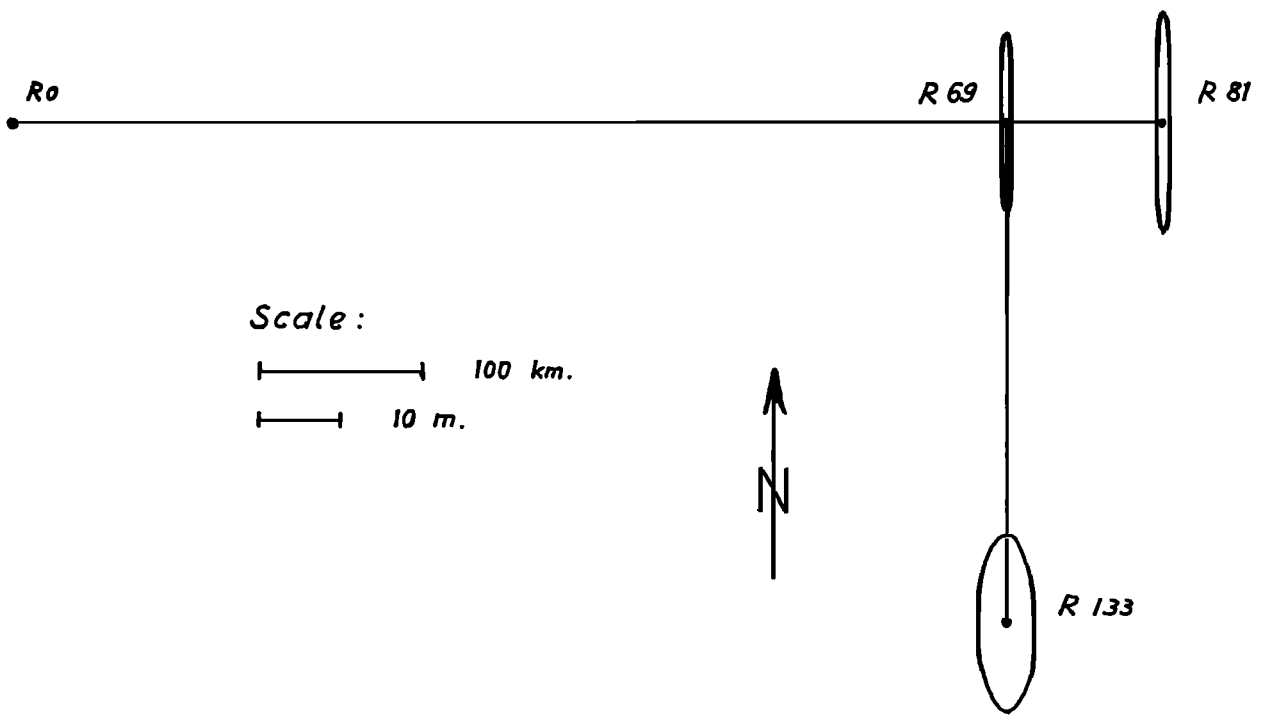

Fig. 13. Error ellipses at three RISS stations.

TABLE 6. List of Geographical Coordinates, Azimuths, and Horizontal Distances at the International Earth Ellipsoid for the RISS Profiles West-East (Dawson Trail) and North-South

Column 1, station and date of measurement during the RISS campaign 1962–1963; column 2, south latitude φ in degrees; column 3, longitude λ in degees; column 4, azimuth α_1 in centesimal degrees, horizontal distance s at sea level, and counterazimuth α_2, in centesimal degrees.

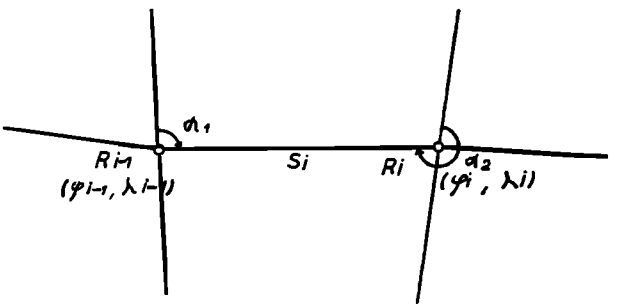

Profile West-East (Dawson Trail)

1	2			3			4
Station and date	φ, deg.	min.	sec.	λ, deg.	min.	sec.	α_1, s, α_2
C. A.	77	50	52.5	166	40	13.8	
							162.6999
10/25/62							741.33
							362.6810
O. H.	77	51	12 4	166	41	16.6	
							124.9719
11/02							24,653.47
							323.9115
R1	77	56	10.2	167	39	50.2	
							122.1622
11/06							7,676.65
							321 8256
R2	77	57	34.0	167	58	25.3	
							121.5433
11/06							8,169 41
							321.1832
R3	77	59	00 7	168	18	18.4	
							118 0121
11/06							7,091.21
							317.6933
R4	78	00	04.0	168	35	54.2	
							119.7006
11/07							7,190.75
							319 3795
R5 = M435	78	01	14.1	168	53	37.9	
							155.3231
11/09							8,119.74
							355.0762
R6	78	04	33.7	169	07	15.7	
							155.0894
11/09							8,189.13
							354.8380
R7	78	07	54.4	169	21	07 9	
							154.6418
11/09							8,122.98
							354.3893

TABLE 6. (Continued)

1	2			3			4
Station and date	φ, deg.	min.	sec.	λ, deg.	min.	sec.	α_1 s, α_2
R8 = M420	78	11	12 2	169	35	04 0	
							154 0722
11/10							9,718.48
							353 7652
R9	78	15	07.0	169	52	00 1	
							154 2709
11/10							10,929.46
							353 9246
R10	78	19	31.7	170	11	05 9	
							154 2283
11/11							11,900.88
							353.8483
R11 = M400	78	24	19.7	170	32	03.0	
							153 3525
11/11							10,630.53
							353.0055
R12	78	28	33.8	170	51	10.3	
							153 3159
11/11							10,576.42
							352 9684
R13	78	32	46.6	171	10	19.4	
							153.1023
11/12							11,547.77
							352 7188
R14 = M380	78	37	21.6	171	31	27.1	
							152.3229
11/12							11,385 80
							351.9371
R15	78	41	49.7	171	52	42.0	
							152.2871
11/13							10,615 38
							351.9249
R16	78	45	59.6	172	12	38.6	
							152 1504
11/13							10,821.00
							351 7779
R17 = M360	78	50	13.8	172	33	08.8	
							115.0602
11/14							8,328 06
							314.6514
R18	78	51	15 9	172	55	38.8	
							114 3429
11/14							8,251.13
							313.9362
R19	78	52	14.5	173	18	01.9	
							113.7337
11/15							8,191.09
							313 3285
R20	78	53	10.2	173	40	19.8	
							113.7209
11/16							7,940 03
							313.3275
R21 = M340	78	54	04.2	174	01	58.6	
							112.5968
11/18							4,948.89
							312.3506
R22	78	54	35.2	174	15	31 7	
							112.8379
11/19							9,107.94
							312.3843

TABLE 6. (Continued)

1	2			3			4
Station and date	φ, deg.	min.	sec.	λ, deg.	min.	sec.	α_1, s, α_2
R23	78	55	33 0	174	40	29.2	
							112 3896
11/19							9,316.81
							311.9243
R24	78	56	30 1	175	06	05.3	
							112.0352
11/20							9,339 84
							311 5676
R25 = M320	78	57	25.6	175	31	49 1	
							111.3558
11/20							8,346.23
							310 9366
R26	78	58	12.4	175	54	52.9	
							110 8837
11/20							8,253 03
							310 4681
R27	78	58	56.8	176	17	44.6	
							110.6598
11/20							8,189.57
							310.2467
R28	78	59	40.0	176	40	28.0	
							110.3760
11/21							7,862.62
							309.9788
R29 = M300	79	00	20.4	177	02	19.3	
							109.8432
11/21							8,487.99
							309.4132
R30	79	01	01.6	177	25	58.3	
							109 5945
11/21							8,178.33
							309.1796
R31	79	01	40 3	177	48	47.6	
							109.2132
11/21							7,748.31
							308.8194
R32	79	02	15 6	178	10	27.2	
							108.5879
11/21							8,453.11
							308.1573
R33 = M280	79	02	51 3	178	34	08.3	
							108 5420
11/22							8,316.94
							308.1179
R34	79	03	26.3	178	57	27.9	
							107.9694
11/22							8,254 80
							307 5476
R35	79	03	58 7	179	20	39.7	
							107.4879
11/22							8,078.66
				+			307.0745
R36	79	04	28.4	179	43	24 2	
						E	107 0134
11/23							8,109.96
				−			306 5976
R37 = M260	79	04	56 3	179	53	44 0	
						W	106.4980
11/23							6,173.80
							306.1811

TABLE 6. (Continued)

1	2			3			4
Station and date	φ, deg.	min.	sec.	λ, deg.	min.	sec.	α_1, s, α_2
R38	79	05	16.1	179	36	18 2	
							106 3294
11/30							10,175 20
							305 8065
R39	79	05	47.3	179	07	32.9	
							106 0704
12/01							9,057 26
							305.6044
R40	79	06	14 0	178	41	55.4	
							105 6240
12/02							7,272.65
							305.2495
R41 = M240	79	06	34.0	178	21	19.5	
							103.5706
12/03							8,270 62
							303 1434
R42	79	06	48.1	177	57	50.2	
							103 0143
12/03							8,139.70
							302.5936
R43	79	06	59.7	177	34	42.2	
							102 6563
12/03							8,272.15
							302.2286
R44	79	07	09.9	177	11	10 8	
							102 1469
12/04							8,063 16
							301 7297
R45 = M220	79	07	17.8	176	48	14 5	
							101 8930
12/04							8,356 05
							301 4605
R46	79	07	24.9	176	24	27.7	
							101 3676
12/04							8,183.47
							300.9440
R47	79	07	29.7	176	01	09 9	
							100.9180
12/05							7,843 28
							300.5118
R48	79	07	32 5	175	38	49 9	
							100 5308
12/05							8,408 15
							300.0954
R49 = M200	79	07	33.9	175	14	53 3	
							99 5641
12/05							8,303 93
							299 1341
R50	79	07	31.1	174	51	14 6	
							99.1053
12/05							8,178 80
							298 6818
R51	79	07	26.5	174	27	57.5	
							98 6642
12/06							7,167 67
							298 2932
R52	79	07	21.0	174	07	33 5	
							98 3290
12/06							9,147 55
							297 8557

TABLE 6. (Continued)

1	2			3			4
Station and date	φ, deg.	min.	sec.	λ, deg.	min.	sec.	α_1, s, α_2
R53 = M180	79	07	12 2	173	41	31 9	
							76 9186
12/06							8,231 08
							276 5212
R54	79	05	37 3	173	19	40 8	
							75 9724
12/06							8,257 01
							275.5771
R55	79	03	58 4	172	57	56.4	
							75 6662
12/07							8,197 74
							275 2755
R56	79	02	19 1	172	36	27.0	
							75 2107
12/07							8,174.53
							274 8232
R57 = M160	79	00	38 3	172	15	08 2	
							85.2533
12/07							8,347.47
							284.8378
R58	78	59	35 6	171	52	16.6	
							84.8060
12/07							8,257.77
							284 3962
R59	78	58	31.9	171	29	44 1	
							84.3845
12/08							8,125.22
							283 9827
R60	78	57	27.4	171	07	37.6	
							83 8335
12/08							8,195.60
							283.4298
R61 = M140	78	56	20.3	170	45	24.8	
							83.3143
12/08							8,209.58
							282.9115
R62	78	55	10.9	170	23	15 0	
							82.9343
12/09							7,536 96
							282.5657
R63	78	54	05.8	170	02	58.0	
							82.4665
12/09							9,624 50
							281.9977
R64	78	52	40 3	169	37	10.2	
							82.1692
12/09							7,494.32
							281.8053
R65 = M120	78	51	32.9	169	17	08 7	
							81.7147
12/10							7,887.74
							281.3333
R66,	78	50	20.1	168	56	09.0	
							81.2615
12/10							8,560 63
							280.8492
R67	78	48	59.2	168	33	27 5	
							80.8889
12/10							8,210.74
							280.4950

TABLE 6. (Continued)

1	2			3			4
Station and date	φ, deg.	min.	sec.	λ, deg.	min.	sec.	α_1, s, α_2
R68 78		47	40 1	168	11	46 5	
							80 5982
12/10							8,167 12
							280.2078
R69 = M100	78	46	20 3	167	50	16 7	
= R100							80 1235
01/16/63							8,790 23
							279.7051
R70	78	44	52.4	167	27	14 8	
							79 7701
01/16							8,224 30
							279.3803
R71	78	43	28.7	167	05	46 9	
							79.4481
01/16							7,889.87
							279.0755
R72	78	42	07.3	166	45	15.8	
							79 1787
01/16							8,665.56
							278 7709
R73 = M80	78	40	36 7	166	22	48.6	
							78.8759
01/17							8,445.92
							278.4801
R74	78	39	07.2	166	01	00 5	
							78 5656
01/17							8,206.05
							278.1824
R75	78	37	39.1	165	39	54.4	
							85.8320
01/17							9,123.65
							285 3926
R76	78	36	33.1	165	15	42 0	
							113 6366
01/17							7,401.38
							313 2790
R77 = M59	78	37	23 2	164	56	00.2	
							82.9486
01/19							7,831.13
							282.5759
R78	78	36	15.7	164	35	28.2	
							87.2563
01/19							7,895.79
							286 8748
R79	78	35	24.3	164	14	27.4	
							44 4235
01/19							3,176.54
							244.3231
R80	78	34	05.8	164	08	55.5	
							54.2463
01/20							3,075 01
							254.1326
R81 = Camp Michigan	78	33	00.4	164	02	39.6	
Profile North-South							
R69 = M100	78	46	20.3	167	50	16.7	
= R100						W	199.8900
12/16/62							6,864.42
							399.8894

TABLE 6. (Continued)

1	2			3			4
Station and date	φ, deg.	min.	sec.	λ, deg.	min.	sec.	α_1, s, α_2
R101	78	50	01.6	167	50	14.7	
							200.5534
12/16							7,216 76
							0.5565
R102	78	53	54 3	167	50	25.2	
							200 8602
12/16							10,172.42
							0.8673
R103	78	59	22 2	167	50	48.4	
							198.5211
12/17							11,083.69
							398.5078
R104	79	05	19 5	167	50	04.6	
							200.6177
12/17							8,638.93
							0 6220
R105	79	09	58 0	167	50	19.0	
							200.9660
12/17							9,428.77
							0.9735
R106	79	15	02.0	167	50	43 7	
							198.7293
12/17							9,298.76
							398 7195
R107	79	20	01.7	167	50	11.4	
							203.1865
12/17							9,243.75
							3.2112
R108	79	24	59.3	167	51	32.5	
							200.1176
12/17							9,405.22
							0.1185
R109	79	30	02.6	167	51	35 6	
							195.2009
12/20							9,309.41
							395.1629
R110	79	35	01.8	167	49	30.6	
							205.5143
12/20							9,585 28
							5.5596
R111	79	40	09.7	167	51	59.7	
							198.2580
12/20							9,354.98
							398.2439
R112	79	45	11.2	167	51	13.3	
							198.4887
12/20							9,243.60
							398 4765
R113	79	50	09.1	167	50	33.2	
							201.5506
12/21							9,218.57
							1.5632
R114	79	55	06.2	167	51	14.5	
							200 2224
12/21							8,924.08
							0.2242
R115	79	59	53.9	167	51	20.3	
							201.0186
12/21							9,691.76
							1.0274

TABLE 6. (Continued)

1	2			3			4
Station and date	φ, deg.	min.	sec.	λ, deg.	min.	sec.	α_1, s, α_2
R116	80	05	06 3	167	51	49 4	
							194.6218
12/21							9,420.77
							394.5762
R117	80	10	09 0	167	49	19 3	
							205 7127
12/21							9,415 27
							5.7615
R118	80	15	11.3	167	51	59.9	
							200.4348
12/22							9,158.48
							0.4385
R119	80	20	06.5	167	52	11.9	
							192 6397
12/22							8,781.17
							392.5800
R120	80	24	47.7	167	48	55.9	
							203.3282
12/22							9,604.45
							3 3580
R121	80	29	56.9	167	50	33.9	
							201.1505
12/22							9,414.31
							1.1607
R122	80	35	00 4	167	51	07.4	
							194.7677
12/22							9,626.86
							394.7199
R123	80	40	09.6	167	48	30.3	
							204.7363
12/25							9,247.09
							4.7783
R124	80	45	06.9	167	50	48.1	
							199 3249
12/27							8,896.82
							399.3191
R125	80	49	53.7	167	50	29.1	
							208.4842
12/28							9,254 18
							8.5606
R126	80	54	49.4	167	54	40.0	
							194.6265
12/28							9,422 21
							394.5767
R127	80	59	52.0	167	51	56.4	
							196.1526
12/28							9,383.93
							396.1166
R128	81	04	54.0	167	49	58.6	
							208.0604
12/28							9,424.91
							8.1366
R129	81	09	55.4	167	54	08.3	
							195.1029
12/30							9,226.99
							395.0571
R130	81	14	51.9	167	51	38 1	
							196.7770
01/02/63							9,279.58
							396 7464

TABLE 6. (Continued)

1	2			3			4
Station and date	φ, deg.	min.	sec.	λ, deg.	min.	sec.	α_1, s, α_2
R131	81	19	50 7	167	49	57.7	
01/05							201 0489 9,510 40 1.0592
R132	81	24	57 2	167	50	31 5	
01/05							197 7786 9,516 69 397 7565
R133	81	30	03 8	167	49	19 1	
Leg to Grounded Ice							
R77 = R200	78	37	23 2	164	56	00.2	
01/23							189.3650 9,102.28 389.2897
R201	78	42	12.4	164	51	51.4	

for any distance measured once, if all values with an asterisk remain unconsidered.

Naturally, these mean square errors are only a measure for the internal accuracy of the traverse, without any reference to the changes during the period of measurement.

For the traverse, first of all, errors at its end and node stations are important, relative to the initial station Camp Area with respect to Observation Hill. Due to its nearly linear extension, lateral deviations will be caused only by angle errors, longitudinal deviations only by distance errors. Figure 13 shows the error ellipses for stations R69, R81, and R133. As a result of the unfavorable propagation of errors of the traverse (double summation), lateral errors are essentially bigger than longitudinal ones, even though the absolute values of all distance differences were used instead of the mean square error given above. For the traverse, a final longitudinal error of $0.032\sqrt{81} = \pm 0.3$ meter results from the mean distance error of ± 0.032 meter.

Part 3. Electronic Distance Measurement

K. Nottarp

4. DISTANCE MEASURING EQUIPMENT AND DISTANCE MEASUREMENT

4.1 *Instruments and Instrument Modifications*

As a result of experiences in Greenland during the International Glaciological Greenland Expedition, 1959, and following freezing-chamber tests, the instruments were modified for use on the Ross ice shelf. In addition to the cold temperature, transportation of the instruments on low open sledges over a rough wind-packed snow surface had to be taken into consideration.

A number of capacitors and potentiometers, as well as all cables, were replaced by cold-resistant types, and the lubricant of the cavity control was exchanged for a silicone grease. The instruments MA1-17, MR1-17, and MR1-30 were fitted with aerial connectors and with crystal ovens for the pattern-frequency quartzes. All power packs were replaced by more robust, fully transistorized units of higher efficiency. The montage of some parts was strutted. All instruments were built in light, snow-proof aluminum boxes, stuffed with silicone foam rubber and mounted directly on the Nansen sledges.

4.2 *Separated Aerial System*

The 1959 campaign in Greenland had proved that it was impossible to measure distances longer than 2 km if the line of sight between the two stations came close to, or touched, the snow surface. The signal loss results from two origins: the influence of the dielectric properties of snow on wave propagation along the air-snow boundary, and refraction in the lower air layers with steep temperature gradients over snow. To span longer distances it is therefore necessary for the line of sight to maintain a minimum distance of 1 to 2 meters from the surface between the stations with respect to the Earth curvature and the local topography. Hence it follows that for lines of 8 to 10 km over flat ground an aerial height of at least 3 meters is required. The aerial system was therefore separated from the tellurometer and mounted on a light, easily handled mast of aluminum tubes. Figure 14 shows some construction details. The knee joint on the lower end was for easy insertion of the mast in the marker tube.

It was difficult to find a cable suitable for the connection between the aerial system and the tellurometer. The qualities required for that particular purpose are low loss at 3000 Mc/s, high flexibility under low temperatures, sufficient tensile strength, and resistance against ultraviolet irradiation. To overcome the unavoidable cable loss of 4.5 db, dishes of 620 mm diameter and 150 mm focal length, instead of the normal aerial reflectors of 400

mm diameter were used. An increase in efficiency of 3.5 db for the transmitter and for the receiver path, altogether 7 db, was thus gained. Moreover, the new power pack of the tellurometer was constructed for the highest permissible plate voltage of the klystron oscillator, giving an additional gain of 2 db. To match the cable with the klystron on the one hand and the aerial system on the other, coaxial impedance transformers were used.

4.3 *Frequency Control Instrument*

For the evaluation of tellurometer measurements exact values for the master pattern frequencies are imperative. Under the rough transport conditions,

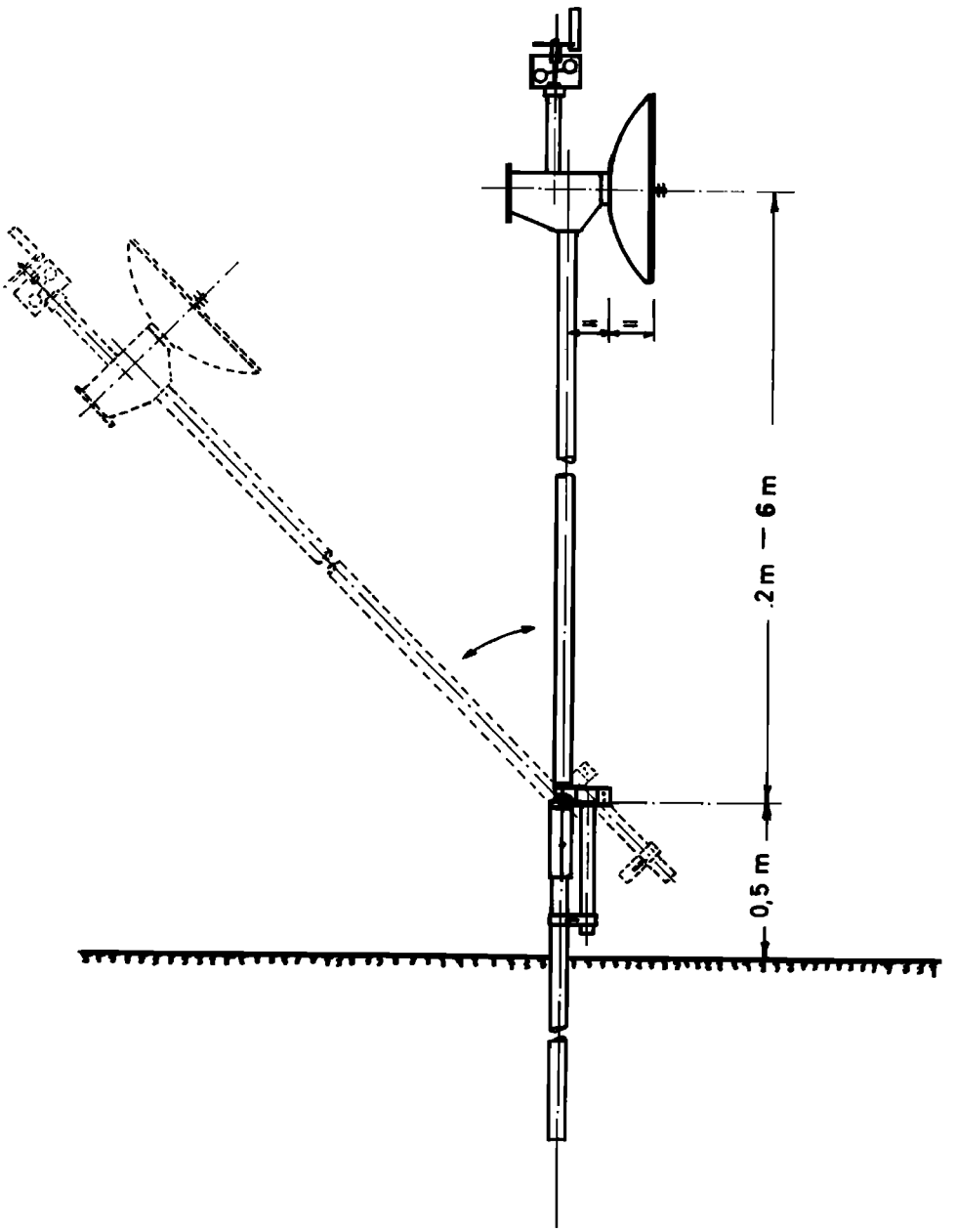

Fig. 14. Mast for separated aerial system.

spontaneous changes of these frequencies were to be expected; therefore a portable frequency-control instrument was constructed for the expedition [*Nottarp,* 1964]. With this instrument the sign and value of deviations of the pattern frequencies from their nominal value can be measured. The drift of the comparison frequency oscillators is checked by an independent built-in reference oscillator. Comparison with standard radio frequencies such as WWV or WWVH was not adopted, because the reception conditions in polar regions often left much to be desired. The instrument also includes a signal generator for the tellurometer, i.e., amplitude and frequency modulated by 1 kc/s and a multimeter. By this means the whole tellurometer instrument can be checked and, if necessary, adjusted. The pattern frequencies of the tellurometers used during the expedition could be controlled within ± 5 c/s equivalent $\pm 5 \times 10^{-7}$ of the nominal value. The frequency drift of the reference oscillator was -10.1 c/s between the checks with the standard of the McMurdo transmitter station before and after the expedition. Jerky frequency changes of the reference oscillator have not appeared during the expedition (see 4.6).

4.4 *Power Supply*

Eight acid accumulators of 12 volts and 42 amp hours were used to supply the instruments. During the expedition two of them failed.

Unfortunately the charging generator broke down after a few days, owing to a flaw in the dynamo. The batteries were therefore charged only with the small toboggan dynamos. The much longer charging times caused some delay in the distance measurements, since for several hours per day the toboggan engines ran as charging generators. They proved good even under this additional wear.

4.5 *Progress of Measurement*

For the distance measurement the aerial mast was put on the marker tube, planted in the snow by group I, erected, and fixed with a tension clamp. To prevent the contacts from icing, the cable connection between tellurometer and aerial system was not disconnected during the journey. The marker tube could be rotated easily in the snow, so that the aerial system could be aligned without difficulty to the respective remote station.

From each station, group II measured the distance to the forward and the backward station with the master tellurometer MA1-17. Between the coarse readings at the beginning and the end of each distance measurement, ten fine readings were executed. Between the forward and the backward measurement, the meteorological observations necessary for the reduction of the measurements were made (see section 6).

The swing was about 2 units and had mostly up to 2 periods. From this the wave propagation and reflection conditions over the Ross ice shelf seem to be a little different from those over the Greenland ice cap.

Originally it was also planned to measure directly the distance between the outer stations (groups I and III) as a check against coarse errors. Therefore group I and group III used the master and remote tellurometers MRA2-MV4 and MRA2-MV3, respectively. The shortage in power supply (see 4.4) prohibited these measurements, but since each distance was measured twice independently, sufficient security exists without the overlapping measurements.

At a wind speed over 2.5 m/s the aerial system was sometimes charged electrostatically. This static occasionally interrupted the measurement momentarily, without further consequences.

During the angle measurement the aerial mast of group II was put in the snow beside the station to release the marker tube for the theodolite without interruption of the radio contact between the groups.

4.6 *Frequency Checks*

Several times during the expedition the pattern frequencies of the tellurometers used were measured with the frequency control instrument described in 4.3. With regard to the frequency drift of the reference oscillator, these checks resulted in the pattern frequency deviation as plotted in Figure 15. The cause of these small deviations may have been small changes in the crystal oven temperature. Spontaneous changes of pattern frequencies appearing as spontaneous shiftings of the pattern frequency differences $A_- - A$ and $A - A_+$ audible during the measurement did not occur. Therefore it seems reasonable to distribute the small frequency deviations between the frequency checks linearly.

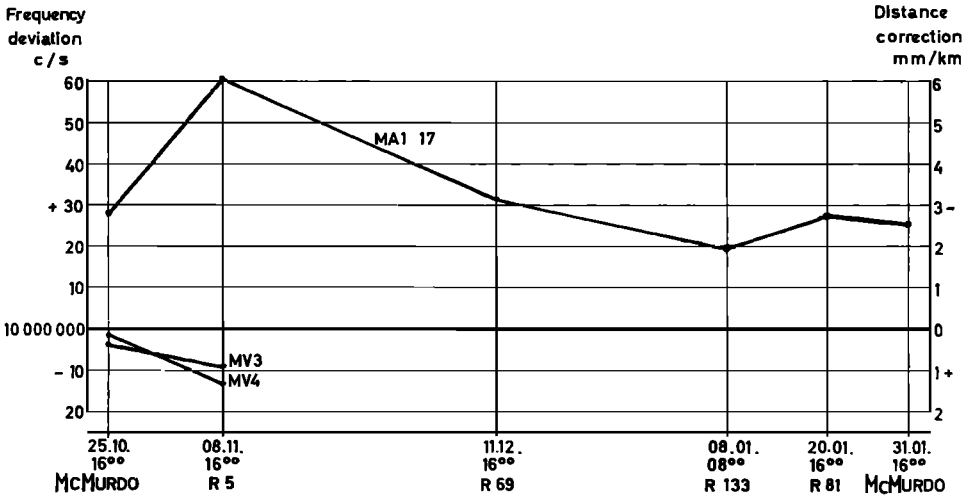

Fig. 15. Frequency deviation during campaign.

5. DIELECTRIC MEASUREMENTS ON SNOW

5.1 *Aim and Arrangement of Measurement*

The expedition provided an opportunity to make some studies on electromagnetic wave propagation at a frequency of about 3000 Mc/s. This investigation should clarify possible influences of the air-snow boundary on the propagation of the 3000-Mc/s carrier wave used in the tellurometer system. Beyond that the dielectric properties of snow and air layers close to the snow surface should be measured.

In order to determine the mean refractive coefficient, the tellurometers were installed beneath the snow surface and the transit time of the 3000-Mc/s carrier wave was measured in various depths over known distances between 50 and 250 meters. Attempts were made to measure distances up to 1000 meters in this way, but the signal disappeared in the noise level.

To check these measurements the dielectric constant and the loss factor of undisturbed snow probes from the propagation space have been measured in a special cavity resonator. Density, structure, and temperature of the snow probes have also been measured.

5.2 *Measurements on the Ross Ice Shelf*

In measurements immediately beneath the snow surface in the region of station R69 there appeared a big reflection (swing) caused by a deeper ice layer. The tellurometers were installed immediately beneath this 1.5-cm-thick ice layer. Then the main reflection disappeared; a small residual swing may have been caused by a more distant ice layer, but it may also have been caused by a reflection on the snow-air boundary, moderated by the double passage through the upper ice layer. The relative dielectric constant of snow, calculated from the undisturbed transit time, was in a depth of 18 cm, $\epsilon = 1.66$, and in a depth of 180 cm, $\epsilon = 1.90$.

5.3 *Measurements on the Pole Plateau*

In the glaciological area near the South Pole station similar measurements were executed. With measurements directly beneath the snow surface no reflection occurred. The relative dielectric constant in a depth of 18 cm was $\epsilon = 1.86$.

5.4 *Conclusions*

The evaluation of these measurements is not yet completed; the interpretation of the measured data requires time, because material for comparison is still rare. It seems possible to use the method for determination of mean snow density values, for location of ice layers in snow, and finally for quantitative measurement of undisturbed snow drift.

6. WEATHER OBSERVATIONS ON THE ROSS ICE SHELF

The meteorological observations necessary for the reduction of tellurometer distances were made during stops caused by weather conditions or delayed

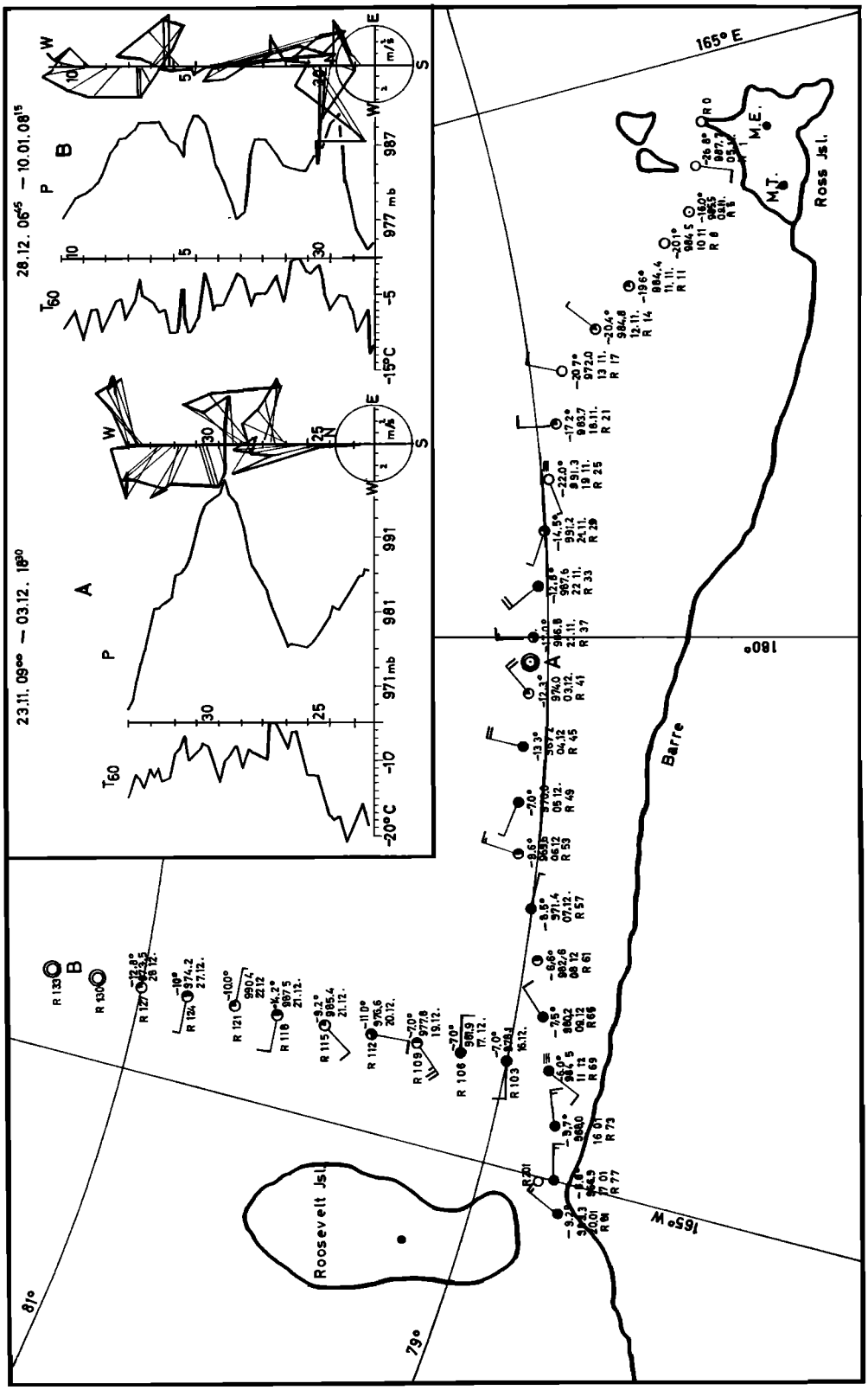

Fig. 16. Weather profile along expedition route.

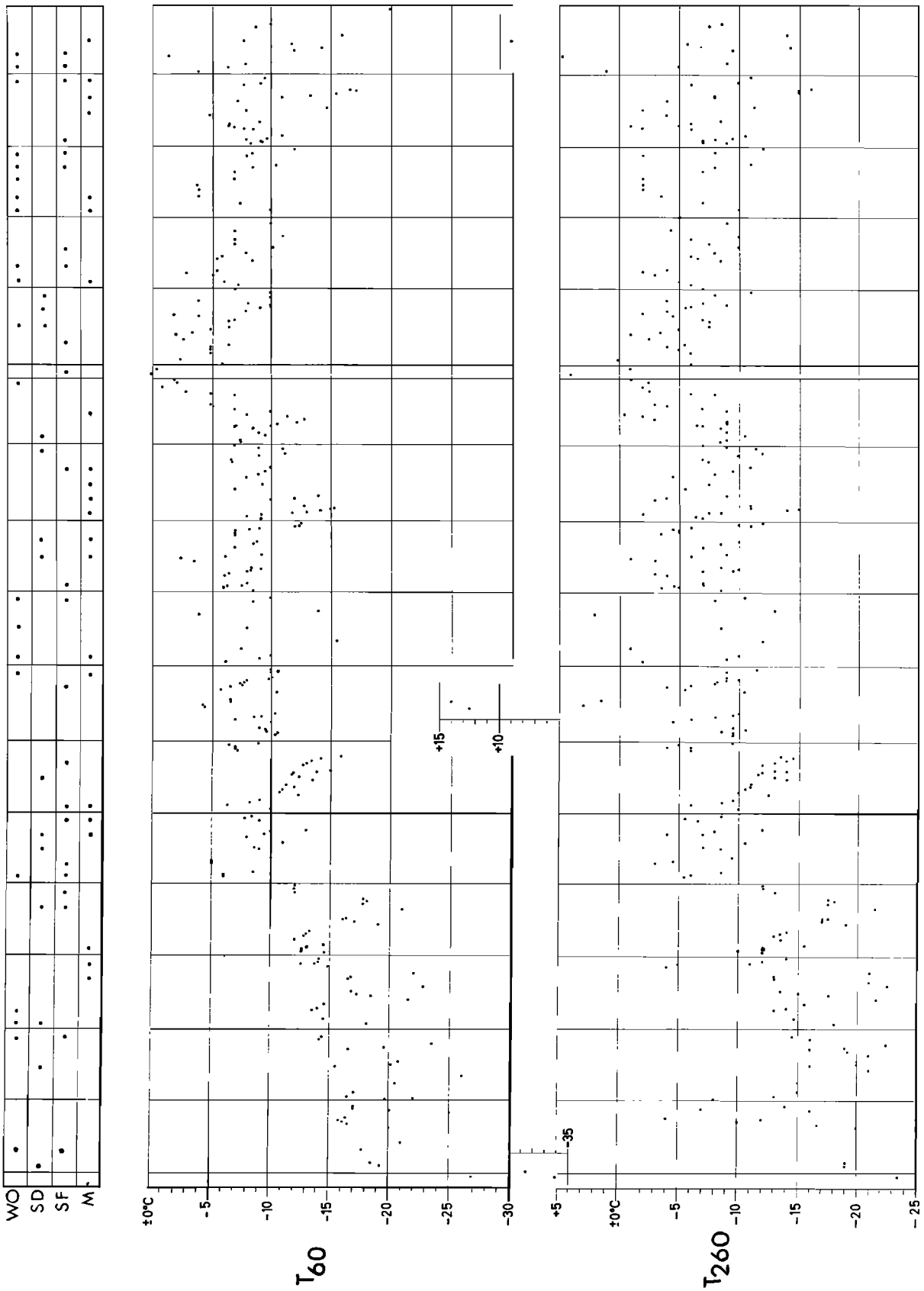

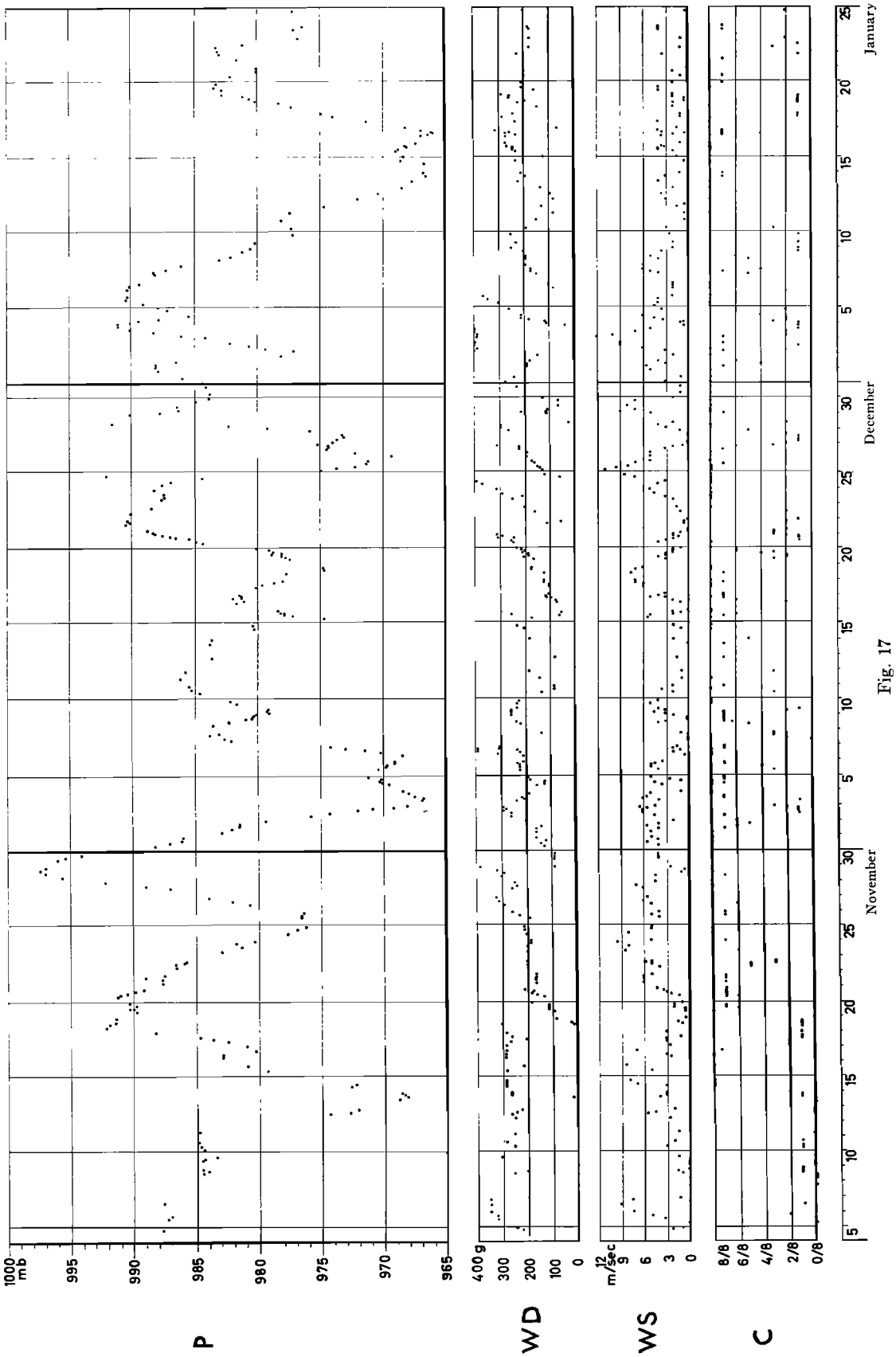

Fig. 17

P, air pressure.
WD, wind direction.
WS, wind speed.
C, cloud coverage.

M, mist or fog.
T_{60}, temperature 60 cm above surface.
T_{260}, temperature 260 cm above surface.

WO, whiteout.
SD, snow drift.
SF, snow fall.

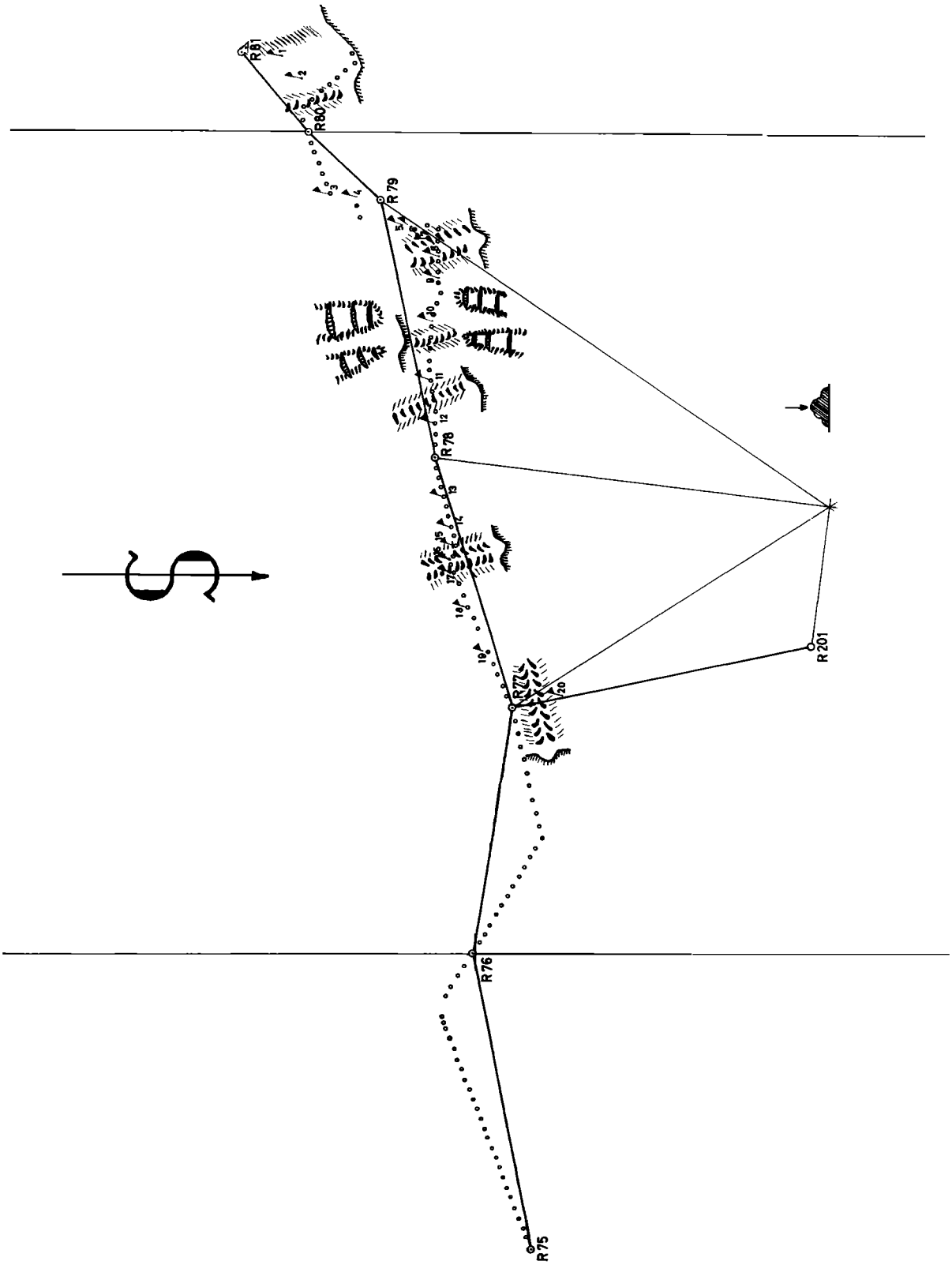

Fig. 18. Expedition route and markers between R75 and R81. The scale is ~1 : 171400.

TABLE 7

T_{60}, temperature 60 cm above surface.
P, air pressure.
WS, wind speed.
WD, wind direction.
C, cloud coverage.
PC, precipitation.

Date	T_{60}, °C	P, mb	WS, m/sec	WD, g	C/8	PC
11/05/62	−30 4	987.7	02 0	235	0	
11/06	−21 9	986 2	04 5	335	1	SD
11/07	−17 8	987.7	03.0	275	1	SD
11/08	−21 0		0		0	
11/09	−17.9	984 6	00 5	230	1	
11/10	−19.5	984 0	00.5	300	0	
11/11	−18 8	984.6	01 0	270	1	
11/12	−23.2	984 8	01 0	250	1	
11/13	−19.4	973 0	04.0	245	0	SD
11/14	−20 0	968 6	03 5	305	1	
11/15	−14.5	972 4	05 0	280	8	SD
11/16	−16.2	980 1	06 5	250	8	SD
11/17	−14 0	982 0	04 0	280	8	
11/18	−20.3	983 9	02.5	260	1	
11/19	−19.0	991.6	01 0	170	1	M
11/20	−13.8	990 0	01 0	120	7	M
11/21	−13 4	990.3	03.0	090	7	M
11/22	−12 8	987.9	06 0	160	7	
11/23	−17.1	986 0	05 0	200	4	
11/24	−18.8	982.0	09.0	190	7	SD
11/25	−13 4	977 7	06 0	000	8	SF
11/26	−6.8	976 4	04 5	360	7	SF
11/27	−5 0	982 2	05 5	300	7	SF
11/28	−9 5	989 0	06 0	250	8	SD
11/29	−10.1	996.6	02.0	350	8	SD
11/30	−8 1	995.1	04 0	090	8	SF
12/01	−8 4	986 8	04 5	130	8	SF
12/02	−11 4	981.4	04.0	170	6	
12/03	−13 0	971.6	05.5	270	2	SD
12/04	−13 4	967.4	04 5	370	6	SF
12/05	−7.3	970 2	03 5	150	7	
12/06	−9.8	969 5	04.5	220	5	
12/07	−9.0	971.4	01 5	320	8	
12/08	−5 6	982.7	0		2	
12/09	−7.6	981.4	02.0	230	7	SF
12/10	−9 3	980 2	04 0	240	6	
12/11	−8.4	985.0	02.5	100	6	
12/12	−11 5	985 9	00.5	160	5	
12/13	−8 0	983 6	01 5	080	7	
12/14	−4 0	983.7	0		7	
12/15	−10 8	981 4	01 5	340	7	SF
12/16	−6 8	977.9	03.0	380	8	SF
12/17	−7 8	981.4	03.0	090	6	
12/18	−5.4	979.0	06 5	110	8	SD
12/19	−8.1	975.6	07.0	160	8	SD
12/20	−8.9	978 2	02 5	020	4	
12/21	−11 1	985 0	02 0	270	3	
12/22	−13.2	989 3	01 0	020	2	
12/23	−8.2	989.2	01 0	170	5	
12/24	−9.1	987.6	04 0	260	8	SF
12/25	−8.4	987.6	05 5	040	8	SD
12/26	−8.4	972 6	08 0	140	8	SD
12/27	−9 1	973.2	03 0	380	6	SD
12/28	−10 9	973 9	01 0	260	2	
12/29	−5 7	984 2	03.0	330	6	

TABLE 7. (Continued)

Date	T_{60}, °C	P, mb	WS, m/sec	WD, g	C/8	PC
12/30	−3 6	987.0	07 0	090	8	SD
12/31	−0 8	983 9	01 5	380	8	SF
01/01/63	−4 5	986 0	03 0	370	8	
01/02	−4 8	985 1	03 5	180	6	SF
01/03	−4 3	979 8	06 5	390	6	SF
01/04	−5 5	987 9	07 0	000	3	SD
01/05	−8 5	988 4	03 0	380	2	SD
01/06	−7 6	989 4	03 5	320	8	
01/07	−4 6	989.9	02 5	090	8	SF
01/08	−7 0	987 4	05 0	170	6	SD
01/09	−8 8	981.7	03 5	100	3	SD
01/10	−8.5	978 2	01 5	240	1	
01/11	−10 0	977 6	01.5	170	6	
01/12	−5 8	976.0	01 0	100	8	
01/13	−4 9	970 2	03.0	100	8	
01/14	−8 6	966.9	03 0	340	7	SF
01/15	−8.2	968 0	00 5	230	8	SF
01/16	−9.6	968 2	02.5	290	8	SF
01/17	−7 3	966.4	02 5	270	7	
01/18	−9.2	972 0	02 0	310	4	
01/19	−11.8	979 0	01.5	000	3	
01/20	−12.7	982.5	03 0	320	4	SF
01/21	−6.7	981 8	01.5	060	7	SF
01/22	−7 2	981.5	03 5	220	5	SF
01/23	−12.5	981 0	01 0	170	2	
01/24	−9 4	976 6	04.0	150	7	
01/25	−20 0	977.1	00 5	200	2	

supply. Hence, from November 5, 1962, to January 25, 1963, almost complete values of air temperature at 60 and 260 cm above the snow surface, air pressure, wind speed, wind direction, cloud coverage, and qualitative items of precipitation are available.

The air temperature at 60 cm above surface was measured with a calibrated Assmann aspirated psychrometer. The air pressure was measured with two Fuess aneroid barometers. They were controlled with the expedition's four other barometers as often as possible and checked with the station barometer at McMurdo at the beginning and end of the traverse. For the measurement of air temperature, wind speed, and wind direction 260 cm above surface a combined instrument, mounted on the aerial mast of the tellurometer, was used. It consisted of a six-cup anemometer, a wind vane, and a thermistor, connected by a multiwire silicone cable to the meter instrument mounted on the sledge. The radiation shield of the thermistor was sometimes obstructed from blowing snow; therefore its indications are not always correct. The wind direction was measured in relation to the

backward traverse site and later converted to north.

Table 7 gives the daily mean values, and Figure 16 shows the weather profile along the expedition route and the development for two stations with longer stops. In Figure 17 all measured meteorological data in chronological sequence are plotted. All times are given in McMurdo station time.

7. EXPEDITION ROUTE BETWEEN R75 AND R81

On the east-west profile the expedition followed the Dawson trail between R1 and R75. This trail was last traveled and marked with bamboo poles by C. Swithinbank in 1959–1960. Some valley systems between R75 and R81 forced us to leave this marked route. Figure 18 shows the situation along this tract. Insofar as recognizable the positions of old bamboos are drawn in, as well as the positions of the RISS aluminum marker tubes and of the twenty new bamboos planted by group III. A big ice rift south of the trail was measured by intersection from the stations R77, R78, R79, and R201.

Acknowledgments. Preparations for this expedition were made at the Glacial Geology and Polar Research Laboratory at the University of Michigan under the direction of Charles W. M. Swithinbank.

This research was supported by the U. S. Antarctic Research Program of the National Science Foundation.

REFERENCES

Brocks, K., Eine räumlich integrierende optische Methode für die Messung vertikaler Temperaturgradienten und Wasserdampfgradienten in der untersten Atmosphäre, *Archiv Meteorol. Geophys. Bioklimatol., Ser. A, 6,* 1954.

Crary, A. P., E. S. Robinson, H. F. Bennet, and W. W. Boyd, Jr., Glaciological studies of the Ross ice shelf, Antarctica, 1957–1960, *IGY Glaciological Rept. 6,* 193 pp., May 1962.

Geiger, R., Das Klima der bodennahen Luftschicht, Braunschweig, 1961.

Hofmann, W., Die geodätische Lagemessung während der Sommerkampagne 1959 der Int. Glaziologischen Grönland-Expedition (EGIG), *Meddelelser om Grönland,* 1964.

Kasten, F., Über die Sichtweite im polar Whiteout, *Polarforschung,* Heft 1/2, 1960.

Miller, L. D., Scintillation and the surveyor, *J. Surveying Mapping Div.,* February 1963.

Nottarp, K., Frequenzkontroll- und Prüfgerät für Tellurometer, *Allgem. Vermessungsnachrichten,* Heft 3, 1964.

Smithsonian Meteorological Tables, 6th revised ed., p. 350, The Smithsonian Institution, Washington, D. C., 1939.

Zumberge, J. H., M. Giovinetto, R. Kehle, and J. Reid, *Deformation of the Ross Ice Shelf near the Bay of Whales, Antarctica,* 148 pp., Geographical Society, New York, 1960.